

An exact solution of the Dirac equation with CP violation

Tomislav Prokopec^{a*}, Michael G. Schmidt^{b*} and Jan Weenink^{a,c*}

^a *Institute for Theoretical Physics (ITP) & Spinoza Institute,
Utrecht University, Postbus 80195, 3508 TD Utrecht, The Netherlands*

^b *Institut für Theoretische Physik, Heidelberg University,
Philosophenweg 16, D-69120 Heidelberg, Germany and*

^c *Nikhef, Science Park Amsterdam 105, 1098 XG Amsterdam, The Netherlands*

We consider Yukawa theory in which the fermion mass is induced by a Higgs like scalar. In our model the fermion mass exhibits a temporal dependence, which naturally occurs in the early Universe setting. Assuming that the complex fermion mass changes as a tanh-kink, we construct an exact, helicity conserving, CP-violating solution for the positive and negative frequency fermionic mode functions, which is valid both in the case of weak and strong CP violation. Using this solution we then study the fermionic currents both in the initial vacuum and finite density/temperature setting. Our result shows that, due to a potentially large state squeezing, fermionic currents can exhibit a large oscillatory magnification. Having in mind applications to electroweak baryogenesis, we then compare our exact results with those obtained in a gradient approximation. Even though the gradient approximation does not capture the oscillatory effects of squeezing, it describes quite well the averaged current, obtained by performing a mode sum. Our main conclusion is: while the agreement with the semiclassical force is quite good in the thick wall regime, the difference is sufficiently significant to motivate a more detailed quantitative study of baryogenesis sources in the thin wall regime in more realistic settings.

PACS numbers: 98.80.-k, 04.62.+v

I. INTRODUCTION

Electroweak baryogenesis [1] is a very appealing idea, and yet the mechanism for dynamical baryon creation at the electroweak scale has suffered some serious blows. Firstly, in the mid 90s it was found that the electroweak phase transition in the standard model is a crossover [2–4]. While at first supersymmetric extensions looked promising, the most popular supersymmetric model - the MSSM - is almost ruled out on two grounds (a) it cannot give a strong enough phase transition for the observed Higgs mass [5] and (b) it cannot produce enough baryons consistent with electric dipole moment [6] bounds [7–12] (albeit in some models resonance between fermionic flavors can be helpful to increase baryon production [10, 13–15]). The models that are still viable are the supersymmetric models with additional Higgs singlet(s) [16, 17] both because they allow for a stronger phase transition [18–20] and generate more baryons [21–25]. In addition, general two Higgs doublet models [26, 27] and composite Higgs models [28–30] are still viable. Works on cold electroweak baryogenesis [31–33] are also worth mentioning. In summary, while electroweak baryogenesis has been a very attractive proposal, precisely because it is testable by contemporary accelerators, recent experiments have cornered it to models where most researchers have not focused their attention during the pre-LHC era. Hence, at this stage theoretical work, that will refine our ability to make a quantitative assessment of electroweak baryogenesis in different models, is still a worthy pursuit.

One of the most important unsolved problems in dynamical modeling of electroweak baryogenesis is a reliable calculation of the CP-violating sources that bias sphaleron transitions [34, 35], which at high temperatures violate baryon number. In the fermionic sector the most prominent CP-violating source is the fermionic axial vector current [36, 37], since that current directly couples to sphalerons, and can thus bias baryon production. There are essentially two approximations used in literature to calculate axial vector currents:

- (a) the quantum-mechanical reflection [38–40] used in the *thin wall* case, and

*T.Prokopec@uu.nl; M.G.Schmidt@thphys.uni-heidelberg.de; J.G.Weenink@uu.nl

(b) the semiclassical force [11, 36, 37, 41–43] used in the *thick wall* case.

In general thin wall baryogenesis is more efficient in producing baryons. Its main drawback is that the calculational methods used are unreliable: one calculates the CP-violating reflected current ignoring the plasma, and then inserts it into a transport equation in an intuitive (but otherwise rather arbitrary) manner [40]. How bad the situation can get is witnessed by the controversy that developed around the work of Farrar and Shaposhnikov [44] (who used a quantum mechanical reflection to calculate the source). The subsequent works [45–47] came up with an orders of magnitude smaller answer for baryon production. And yet these latter works used unreliable methods that *e.g.* violate unitarity, such that the issue remained unsettled¹. So, the problem of the source calculation in the thin wall regime remains still to a large extent open.

In the thick wall case the situation became much more satisfactory after the works of Joyce, Kainulainen, Prokopec, Schmidt and Weinstock [43, 48, 49]. It was shown that one can calculate the semiclassical force (which rather straightforwardly sources the axial vector current) from first principles and in a controlled approximation from the Kadanoff-Baym (KB) equations for Wightman functions. These KB equations are the quantum field theoretic generalization of kinetic equations. The positive and negative frequency Wightman functions represent the quantum field theoretic generalization of the Boltzmann distribution function, that provide statistical information on both on-shell and off-shell phase space flow. In a certain limit, when integrated over energies, the Wightman functions yield Boltzmann's distribution function. When written in a gradient approximation, the KB equations can be split into the constraint equations (CE) and the kinetic equations (KE). The authors of Refs. [48, 49] have rigorously shown that, in the presence of a moving planar interface, in which fermions acquire a mass that depends on one spatial coordinate, single fermions live on a shifted energy shell, which to first order in gradients (linear in \hbar) and in the wall frame equals

$$\omega_{\pm s} = \omega_0 \mp \hbar s \frac{|m|^2 \partial_z \theta}{2\omega_0 \sqrt{k_\perp^2 + |m|^2}}, \quad \omega_0 = \sqrt{\vec{k}^2 + |m|^2}, \quad (1)$$

where $m(z) = m_R(z) + im_I(z) = |m|(z)e^{i\theta(z)}$ is the fermion mass, which varies in the z -direction in which the wall moves, \vec{k} is particle's momentum, \vec{k}_\perp is the momentum orthogonal to the wall, and $s = \pm 1$ is the corresponding spin. This energy shift acts as a pseudo-gauge field (also known from condensed matter studies), which lowers or increases particle's energy. Relation (1) clearly shows that particles with a positive spin orthogonal to the wall and a positive frequency (as well as particles with a negative spin and a negative frequency) will feel a semiclassical force that is proportional to the gradient of $\theta = \arg[m]$. Particles with a negative spin and a positive frequency will feel an opposite force. This force appears in the kinetic equation for the Boltzmann-like distribution functions $f_{\pm s}$, and reads

$$F_{\pm s} = -\frac{\partial_z |m|^2}{2\omega_{\pm s}} \pm \hbar s \frac{\partial_z (|m|^2 \partial_z \theta)}{2\omega_0 \sqrt{k_\perp^2 + |m|^2}}. \quad (2)$$

It was also shown that this force then sources an axial vector current, which in turn can bias sphalerons.

The work of [12, 47, 50–52] has shown that, in the case that fermions mix through a mass matrix, there is an additional CP-violating source resulting from flavor mixing. This was put on a more formal ground by [15], where a flavor independent formalism was developed, and where it was shown that flavor non-diagonal source is subject to flavor oscillations induced by a commutator term of the form $i[M, f]$, not unlike the famous flavor (vacuum) oscillations of neutrinos. This idea was further developed by [53]. Since we do not deal with flavor mixing in this work, we shall not further dwell on this mechanism, which should not diminish its importance. In passing we just mention that in most of the relevant parameter space of *e.g.* the chargino mediated baryogenesis in the MSSM, the semiclassical force induces the dominant CP-violating source current [9].

We shall now present a qualitative argument which suggests that in many situations thin wall sources can dominate over the thick wall sources (calculated in a gradient approximation). If true this means that any serious attempt to make a quantitative assessment of baryon production cannot neglect the thin wall contribution. To see why this is so, recall that a gradient approximation applies for those plasma excitations whose orthogonal momentum, $k_\perp = 2\pi/\lambda_\perp$, satisfies:

$$k_\perp \gg \frac{2\pi}{L} \quad (\text{THICK WALL}), \quad (3)$$

¹ Research on the topic subsided not because the problem was resolved, but because standard model baryogenesis was ruled out based on equilibrium considerations alone [2].

where L is the typical thickness of the bubble wall. On the other hand, the thin wall approximation belongs to the realm of momenta which satisfy

$$k_{\perp} \leq \frac{2\pi}{L} \quad (\text{THIN WALL}). \quad (4)$$

Typical momenta of particles in a plasma (per direction) is $k_{\perp} \sim T$. Now, unless $LT \gg 2\pi$, we have a larger or comparable number of particles in the thin and thick wall regimes! But, since the thin wall source is typically stronger, unless thermal scattering significantly suppress the thin wall source, it will dominate over the thick wall source. It is often incorrectly stated in literature that the number of particles to which thin wall calculation applies is largely phase space suppressed, *i.e.* that their number is small when compared to the number of particles to which the semiclassical treatment applies. So, to conclude, it is of essential importance to get the thin wall source right if we are to claim that we can reliably calculate baryon production at the electroweak transition in a model.

We believe that this represents a good motivation for what follows: a complete analytic treatment of fermion tree-level dynamics for a time dependent mass. The time dependence has been chosen such to correspond to a tanh-kink wall, because it is known that this represents a good approximation to a realistic bubble wall [54, 55], and equally importantly, in this case one can construct exact solutions for mode functions. Before we begin our quantitative analysis, we recall that a related study for the CP even case and planar wall has been conducted by Ayala, Jalilian-Marian, McLerran and Vischer [56], while a semianalytic, perturbative treatment of the CP-violating case has been conducted in Ref. [57]. The main advantage of the latter study is that it allows for a general profile of the CP-violating mass parameter, the drawbacks are that the method is semianalytic (the final expression for the source is in terms of an integral), and furthermore it is perturbative, such that it can be applied to small CP violation only. To conclude, an exact treatment of fermion dynamics in the presence of a strong CP violation is highly desirable, and this is precisely what we do in this paper.

II. THE MODEL

Here we consider the free fermionic lagrangian of the form,

$$\mathcal{L}_0 = \bar{\psi} i \gamma^{\mu} \partial_{\mu} \psi - m^* \bar{\psi}_R \psi_L - m \bar{\psi}_L \psi_R, \quad (5)$$

where $\psi_L = P_L \psi$ and $\psi_R = P_R \psi$ are the left and right handed single fermionic fields, $P_L = (1 - \gamma^5)/2$ and $P_R = (1 + \gamma^5)/2$ are the left and right handed projectors, and γ^{μ} and γ^5 are the Dirac gamma matrices. We shall assume that the fermion mass m is complex and space-time dependent. This can be generated *e.g.* when a Yukawa interaction term, $\mathcal{L}_y = -y \phi \bar{\psi}_L \psi_R + \text{h.c.}$, is approximated by $-y \langle \hat{\phi} \rangle \bar{\psi}_L \psi_R + \text{h.c.}$, where $\langle \hat{\phi} \rangle$ stands for a Higgs-like scalar field condensate which can generate a space-time dependent fermion mass,

$$m(x) = y \langle \hat{\phi}(x) \rangle, \quad (6)$$

where y is a (complex) Yukawa coupling. The Dirac equation implied by (5) is

$$i \gamma^{\mu} \partial_{\mu} \psi - m^* \psi_L - m \psi_R = 0. \quad (7)$$

In this paper we consider the simplest case: a single fermion in a time dependent, but spatially homogeneous, background. Such situations can occur, for example in expanding cosmological backgrounds [58], or during second order phase transitions and crossover transitions in the early Universe. In this case helicity is conserved [59–61]. We shall perform the usual canonical quantization procedure, according to which the spinor operator $\hat{\psi}(x)$ satisfies the following anti-commutator ($\hbar = 1$),

$$\{\hat{\psi}_{\alpha}(\vec{x}, t), \hat{\psi}_{\beta}^{\dagger}(\vec{x}', t)\} = \delta_{\alpha\beta} \delta^3(\vec{x} - \vec{x}'). \quad (8)$$

In the free case under consideration, the Dirac equation (7) is linear, and consequently $\hat{\psi}(x)$ can be expanded in terms of the creation and annihilation operators, which in the helicity basis reads,

$$\hat{\psi}(\vec{x}, t) = \int \frac{d^3 k}{(2\pi)^3} \sum_{h=\pm} \left[e^{i\vec{k} \cdot \vec{x}} \hat{a}_{\vec{k}h} \chi_h(\vec{k}, t) + e^{-i\vec{k} \cdot \vec{x}} \hat{b}_{\vec{k}h}^{\dagger} \nu_h(\vec{k}, t) \right], \quad (9)$$

where $\chi_h(\vec{k}, t)$ and $\nu_h(\vec{k}, t)$ are particle and antiparticle four-spinors. $\hat{a}_{\vec{k}h}$ and $\hat{b}_{\vec{k}h}$ are the annihilation operators that destroy the fermionic vacuum state $|\Omega\rangle$, $\hat{a}_{\vec{k}h} |\Omega\rangle = 0 = \hat{b}_{\vec{k}h} |\Omega\rangle$, while $\hat{a}_{\vec{k}h}^{\dagger}$ and $\hat{b}_{\vec{k}h}^{\dagger}$ are the creation operators that create

a particle and an antiparticle with momentum \vec{k} and helicity h . These operators obey the following anticommutator algebra,

$$\begin{aligned} \{\hat{a}_{\vec{k}h}, \hat{a}_{\vec{k}'h'}^\dagger\} &= \delta_{hh'}(2\pi)^3 \delta^3(\vec{k} - \vec{k}'), & \{\hat{a}_{\vec{k}h}, \hat{a}_{\vec{k}'h'}\} &= 0, & \{\hat{a}_{\vec{k}h}^\dagger, \hat{a}_{\vec{k}'h'}^\dagger\} &= 0 \\ \{\hat{b}_{\vec{k}h}, \hat{b}_{\vec{k}'h'}^\dagger\} &= \delta_{hh'}(2\pi)^3 \delta^3(\vec{k} - \vec{k}'), & \{\hat{b}_{\vec{k}h}, \hat{b}_{\vec{k}'h'}\} &= 0, & \{\hat{b}_{\vec{k}h}^\dagger, \hat{b}_{\vec{k}'h'}^\dagger\} &= 0, \end{aligned} \quad (10)$$

where all mixed anticommutators are zero. The momentum space quantization conditions (10) and the position space quantization rule (8) have to be mutually consistent. This imposes the following consistency condition on the positive and negative frequency spinors,

$$\sum_{h=\pm} [\chi_{h\alpha}(\vec{k}, t) \chi_{h\beta}^*(\vec{k}, t) + \nu_{h\alpha}(-\vec{k}, t) \nu_{h\beta}^*(-\vec{k}, t)] = \delta_{\alpha\beta}. \quad (11)$$

This is usually supplied by the mode orthogonality conditions,

$$\bar{\chi}_h(\vec{k}, t) \cdot \nu_h(\vec{k}, t) = 0 = \bar{\nu}_h(\vec{k}, t) \cdot \chi_h(\vec{k}, t). \quad (12)$$

and by the mode normalization conditions,

$$\chi_h^\dagger(\vec{k}, t) \cdot \chi_h(\vec{k}, t) = 1 = \nu_h^\dagger(\vec{k}, t) \cdot \nu_h(\vec{k}, t), \quad (13)$$

which – as we will see below – are chosen to be consistent with the more general requirement (11). Although the orthogonality condition (12) is usually met, it is however not a necessity. Important is that the mode functions span all of the Hilbert space, which is true in this case. Because we consider a system which is time-translationally invariant, helicity is conserved, and it is thus convenient to work with helicity conserving spinors

$$\chi_h(\vec{k}, t) = \begin{pmatrix} L_h(\vec{k}, t) \\ R_h(\vec{k}, t) \end{pmatrix} \otimes \xi_h(\vec{k}), \quad \nu_h(\vec{k}, t) = \begin{pmatrix} \bar{L}_h(\vec{k}, t) \\ \bar{R}_h(\vec{k}, t) \end{pmatrix} \otimes \xi_h(\vec{k}), \quad (14)$$

where $\xi_h(\vec{k})$ is the helicity two eigen-spinor, satisfying $\hat{h}\xi_h = h\xi_h$, where $\hat{h} = \hat{k} \cdot \vec{\sigma}$ is the helicity operator and $h = \pm 1$ are its eigenvalues.

We shall work here with the Dirac matrices in the chiral representation, in which

$$\gamma^0 = \begin{pmatrix} 0 & I \\ I & 0 \end{pmatrix} = \rho^1 \otimes I, \quad \gamma^i = \begin{pmatrix} 0 & \sigma^i \\ -\sigma^i & 0 \end{pmatrix} = \iota \rho^2 \otimes \sigma^i, \quad \gamma^5 \equiv \iota \gamma^0 \gamma^1 \gamma^2 \gamma^3 = \begin{pmatrix} -I & 0 \\ 0 & I \end{pmatrix} = -\rho^3 \otimes I, \quad (15)$$

where the last equalities follow from the usual direct product (Bloch) representation of the Dirac matrices. Here ρ^i and σ^i are the Pauli matrices obeying, $\rho^i \rho^j = \delta^{ij} + \iota \epsilon^{ijl} \rho^l$ and $\sigma^i \sigma^j = \delta^{ij} + \iota \epsilon^{ijl} \sigma^l$. The left and right projectors are then,

$$P_L = \frac{1 - \gamma^5}{2} = \begin{pmatrix} I & 0 \\ 0 & 0 \end{pmatrix} = \frac{1 + \rho^3}{2} \otimes I, \quad P_R = \frac{1 + \gamma^5}{2} = \begin{pmatrix} 0 & 0 \\ 0 & I \end{pmatrix} = \frac{1 - \rho^3}{2} \otimes I, \quad (16)$$

which can be used to write, $\psi_L = P_L \psi$ and $\psi_R = P_R \psi$ as it is done in (5–7). Now, making use of Eqs. (9–16) in the Dirac equation (7) one gets the following four equations for the component functions

$$\begin{aligned} \iota \dot{L}_h + h k L_h &= m R_h \\ \iota \dot{R}_h - h k R_h &= m^* L_h \end{aligned} \quad (17)$$

and

$$\begin{aligned} \iota \dot{\bar{L}}_h - h k \bar{L}_h &= m \bar{R}_h \\ \iota \dot{\bar{R}}_h + h k \bar{R}_h &= m^* \bar{L}_h, \end{aligned} \quad (18)$$

where the mass can be complex and time dependent, $m = m(t)$, and the modes are normalized to unity,

$$|L_h|^2 + |R_h|^2 = 1 = |\bar{L}_h|^2 + |\bar{R}_h|^2 \quad (19)$$

The equations of motion for L_h and R_h can be decoupled, resulting in the second order equations,

$$\begin{aligned}\ddot{L}_h + \omega^2 L_h - \frac{\dot{m}}{m}(\dot{L}_h - \imath h k L_h) &= 0 \\ \ddot{R}_h + \omega^2 R_h - \frac{\dot{m}^*}{m^*}(\dot{R}_h + \imath h k R_h) &= 0,\end{aligned}\tag{20}$$

where $\omega^2 = k^2 + |m(t)|^2$. For the case at hand a better way of proceeding is to go to the positive and negative frequency basis, defined by:

$$u_{\pm h} = \frac{1}{\sqrt{2}}(L_h \pm R_h), \quad v_{\pm h} = \frac{1}{\sqrt{2}}(\bar{L}_h \pm \bar{R}_h),\tag{21}$$

since then the equation of motion can be reduced to the Gauss' hypergeometric equation. Indeed, from (17–18) and (21) it follows,

$$\begin{aligned}\dot{u}_{\pm h} \mp m_R(t)u_{\pm h} &= -(hk \pm \imath m_I)u_{\mp h} \\ \dot{v}_{\pm h} \mp m_R(t)v_{\pm h} &= (hk \mp \imath m_I)v_{\mp h},\end{aligned}\tag{22}$$

which, when decoupled, yields a second order equation,

$$\ddot{u}_{\pm h} \mp \imath \frac{\dot{m}_I}{hk \pm \imath m_I} \dot{u}_{\pm h} + \left(k^2 + |m|^2 \pm \imath \dot{m}_R + \frac{m_R \dot{m}_I}{hk \pm \imath m_I} \right) u_{\pm h} = 0.\tag{23}$$

So far our analysis has been general, in the sense that we have assumed no special time dependence in $m(t)$. In order to make progress however, we have to make a special choice for $m(t)$, which is what we do next.

III. MODE FUNCTIONS FOR THE KINK PROFILE

In Ref. [56] an exact solution of the Dirac equation was found for a wall of arbitrary thickness with a kink wall profile $\propto \tanh(-z/L)$, where $L \equiv 1/\lambda$ characterizes the wall thickness. Here we generalize this solution to include CP violation. While in this paper we consider only a time dependent mass profile, the generalization to the planar (z -dependent) case is straightforward, and will be considered separately. Constructing an exact solution is important for baryogenesis since one can then consider in detail how the CP-odd quantities that source baryogenesis (directly or indirectly) depend on the mass profile, and in particular investigate what is the optimal profile and its duration. Unfortunately, analytic solutions cannot include plasma scattering and width effects, whose treatment will be therefore typically left to numerical simulations.

Here we assume the following ‘wall’ profile

$$m(t) = m_1 + m_2 \tanh\left(-\frac{t}{\tau}\right),\tag{24}$$

where $\tau \equiv 1/\gamma$ represents the time scale over which the wall varies (for convenience we shall use the terms ‘wall’ and ‘profile’ interchangeably). Both m_1 and m_2 are complex mass parameters. In the case when a single Higgs field is responsible for the phase transition, one expects that both real and imaginary part of $m(t)$ exhibit a similar behaviour, which is reflected in the *Ansatz* (24). Moreover, we do not know how to construct exact solutions when different time scales govern the rate of change of the real and imaginary masses. Nevertheless, we believe that the *Ansatz* (24) represents quite well realistic walls for a wide variety of single stage phase transitions, *cf.* Refs. [54, 55].

Note that the thin wall limit is $\tau \rightarrow 0$ ($\gamma \rightarrow \infty$). In that limit the mass function becomes the step function *Ansatz* (B1), whereby $m_{\pm} = m_1 \mp m_2$. In appendix A we construct the normalized fundamental solutions of Eqs. (17) for a constant mass. The thin wall case is treated explicitly in appendix B. The thin wall results serve as a check for the kink wall case in the appropriate limits. Moreover it allows for a quantitative comparison of the thick wall to the thin wall results.

Since the ratio of the real and imaginary parts of the mass $m_I(t)/m_R(t)$ is time dependent, the *Ansatz* (24) contains CP violation (which can be either small or large, depending on how much the ratio $m_I(t)/m_R(t)$ changes. Since the physical CP-violating phase is in the relative phase between m_1 and m_2 , one can perform a global rotation of the left- and right-handed spinors that does not affect CP violation. It turns out that the equations of motion simplify if one performs a global rotation that removes the imaginary part of m_2 . The constant rotation that does that is

$$m(t) \rightarrow m(t)e^{\imath\chi}, \quad \chi = \arctan\left(-\frac{m_{2I}}{m_{2R}}\right).\tag{25}$$

In that case

$$m_1 = m_{1R} + m_{1I}, \quad m_2 = m_{2R}.$$

This rotation is important, because the mode equations (23) significantly simplify to become

$$\ddot{u}_{\pm h} + (\omega^2(t) \pm i\dot{m}_R)u_{\pm h} = 0, \quad (26)$$

where $\omega^2(t) = k^2 + |m(t)|^2$. Furthermore, from (22) one can infer that $v_{\pm h}$ obey the same equations as $u_{\pm h}$. In what follows, we show that these equations can be reduced to the Gauss' hypergeometric equation.

To show this, it is instructive to introduce a new variable,

$$z = \frac{1}{2} - \frac{1}{2} \tanh\left(-\frac{t}{\tau}\right), \quad (27)$$

in terms of which

$$m(t) = m_1 + m_2(1 - 2z), \quad \dot{m}_R(t) = -2m_{2R}\dot{z} = -\frac{\gamma m_{2R}}{\cosh^2(-t/\tau)} = -4\gamma m_{2R}z(1 - z),$$

with $\gamma = 1/\tau$. Eq. (26) becomes,

$$\left\{ 4\gamma^2 [z(1-z)]^2 \frac{d^2}{dz^2} + 4\gamma^2 (1-2z)z(1-z) \frac{d}{dz} + \left[k^2 + m_I^2 + (m_{1R} + m_{2R})^2 - 4zm_{1R}m_{2R} - 4z(1-z)m_{2R}(m_{2R} \pm i\gamma) \right] \right\} u_{\pm h} = 0. \quad (28)$$

Now, performing a rescaling,

$$u_{\pm h} = z^\alpha (1 - z)^\beta \chi_{\pm h}(z) \quad (29)$$

and choosing

$$\alpha = -\frac{i}{2} \frac{\omega_-}{\gamma}, \quad \beta = -\frac{i}{2} \frac{\omega_+}{\gamma}, \quad (30)$$

where

$$\omega_{\mp} \equiv \omega(t \rightarrow \mp\infty) = \sqrt{k^2 + m_I^2 + (m_{1R} \pm m_{2R})^2}, \quad (31)$$

yields the following Gauss' hypergeometric equation for $\chi_{\pm h}$,

$$\left[z(1-z) \frac{d^2}{dz^2} + [c - (a_{\pm} + b_{\pm} + 1)z] \frac{d}{dz} - a_{\pm}b_{\pm} \right] \chi_{\pm h}(z) = 0, \quad (32)$$

where

$$a_{\pm} = \alpha + \beta + 1 \mp i \frac{m_{2R}}{\gamma}, \quad b_{\pm} = \alpha + \beta \pm i \frac{m_{2R}}{\gamma}, \quad c = 2\alpha + 1. \quad (33)$$

Note that the rescaling (29) was chosen such to remove the terms $\propto 1/z$ and $\propto 1/(1-z)$ from Eq. (32). Since a_{\pm}, b_{\pm}, c are non-integer, the two independent solutions for $\chi_{\pm h}$ are the usual ones. A detailed normalization procedure is provided in Appendix D and the result are the following normalized *early time* mode functions

$$\begin{aligned} u_{+h} &\equiv u_{+h}^{(1)} = \sqrt{\frac{\omega_- + (m_{1R} + m_{2R})}{2\omega_-}} \times z^\alpha (1 - z)^\beta \times {}_2F_1(a_+, b_+; c; z) \\ u_{-h} &\equiv u_{-h}^{(1)} = -\frac{hk - im_I}{\sqrt{k^2 + m_I^2}} \times \sqrt{\frac{\omega_- - (m_{1R} + m_{2R})}{2\omega_-}} \times z^\alpha (1 - z)^\beta \times {}_2F_1(a_-, b_-; c; z). \end{aligned} \quad (34)$$

These functions are valid of course for all times. They are called *early time* mode functions because at early times ($t \rightarrow -\infty$) they reduce to the positive frequency mode functions (D2), and they are normalized as, $|u_{+h}^{(1)}|^2 + |u_{-h}^{(1)}|^2 = 1$, which follows from Eqs. (19) and (21), see also Eq. (D18).

For completeness, we also quote the second pair (D1) of early time solutions,

$$\begin{aligned} u_{+h}^{(2)} &= \sqrt{\frac{\omega_- - (m_{1R} + m_{2R})}{2\omega_-}} \times z^{\alpha+1-c}(1-z)^{\beta+c-a_+-b_+} \times {}_2F_1(1-a_+, 1-b_+; 2-c; z) \\ u_{-h}^{(2)} &= \frac{hk - im_I}{\sqrt{k^2 + m_I^2}} \times \sqrt{\frac{\omega_- + (m_{1R} + m_{2R})}{2\omega_-}} \times z^{\alpha+1-c}(1-z)^{\beta+c-a_--b_-} \times {}_2F_1(1-a_-, 1-b_-; 2-c; z). \end{aligned} \quad (35)$$

Just as before, at early times ($t \rightarrow -\infty$) these solutions reduce to the negative frequency mode functions (D2), and they are also normalized as, $|u_{+h}^{(2)}|^2 + |u_{-h}^{(2)}|^2 = 1$.

An analogous procedure as above yields the following normalized fundamental solutions suitable for *late times*,

$$\begin{aligned} \tilde{u}_{+h}^{(1)} &= \sqrt{\frac{\omega_+ + (m_{1R} - m_{2R})}{2\omega_+}} \times z^{\alpha+1-c}(1-z)^{\beta+c-a_+-b_+} \times {}_2F_1(1-a_+, 1-b_+; 2-\tilde{c}; 1-z) \\ \tilde{u}_{-h}^{(1)} &= -\frac{hk - im_I}{\sqrt{k^2 + m_I^2}} \times \sqrt{\frac{\omega_+ - (m_{1R} - m_{2R})}{2\omega_+}} \times z^{\alpha+1-c}(1-z)^{\beta+c-a_--b_-} \times {}_2F_1(1-a_-, 1-b_-; 2-\tilde{c}; 1-z) \end{aligned} \quad (36)$$

and

$$\begin{aligned} \tilde{u}_{+h}^{(2)} &= \sqrt{\frac{\omega_+ - (m_{1R} - m_{2R})}{2\omega_+}} \times z^\alpha(1-z)^\beta \times {}_2F_1(a_+, b_+; \tilde{c}; 1-z) \\ \tilde{u}_{-h}^{(2)} &= \frac{hk - im_I}{\sqrt{k^2 + m_I^2}} \times \sqrt{\frac{\omega_+ + (m_{1R} - m_{2R})}{2\omega_+}} \times z^\alpha(1-z)^\beta \times {}_2F_1(a_-, b_-; \tilde{c}; 1-z), \end{aligned} \quad (37)$$

while the late time solutions (37) reduce at asymptotically late times to positive and negative frequency solutions $\propto e^{\mp i\omega_+ t}$, respectively, see Eq. (D7).

Now, a general early time solution can be written as a linear combination of the fundamental solutions (34–35); for simplicity we shall take here (34) for the early time solutions. Similarly, general late time solutions are a linear combination of the fundamental late time solutions (36–37),

$$\tilde{u}_{\pm h} = \alpha_{\pm h} \tilde{u}_{\pm h}^{(1)} + \beta_{\pm h} \tilde{u}_{\pm h}^{(2)}, \quad (38)$$

where $\alpha_{\pm h}$ and $\beta_{\pm h}$ are complex functions of \vec{k} (for spatially homogeneous systems they are functions of the magnitude $\|\vec{k}\|$ only) that satisfy the standard normalization condition,

$$|\alpha_{\pm h}|^2 + |\beta_{\pm h}|^2 = 1. \quad (39)$$

Now, upon choosing (34) as the early time solutions and making use of the matching between the general early and late time solutions

$$\tilde{u}_{\pm h}(k, t) = u_{\pm h}(k, t) \quad (40)$$

and of the relation for the Gauss' hypergeometric functions (D3) one gets,

$$\begin{aligned} \alpha_{\pm h} &= \sqrt{\frac{\omega_+[\omega_- \pm (m_{1R} + m_{2R})]}{\omega_-[\omega_+ \pm (m_{1R} - m_{2R})]}} \frac{\Gamma(c)\Gamma(a_{\pm} + b_{\pm} - c)}{\Gamma(a_{\pm})\Gamma(b_{\pm})} \\ \beta_{\pm h} &= \pm \sqrt{\frac{\omega_+[\omega_- \pm (m_{1R} + m_{2R})]}{\omega_-[\omega_+ \mp (m_{1R} - m_{2R})]}} \frac{\Gamma(c)\Gamma(c - a_{\pm} - b_{\pm})}{\Gamma(c - a_{\pm})\Gamma(c - b_{\pm})}. \end{aligned} \quad (41)$$

It can be shown that

$$\begin{aligned} \alpha_{+h} &= \alpha_{-h} \\ \beta_{+h} &= \beta_{-h}. \end{aligned} \quad (42)$$

Useful identities here are

$$\begin{aligned}\omega_- \mp (m_{1R} + m_{2R}) &= \frac{\pm\omega_+^2 \mp (\omega_- \mp 2m_{2R})^2}{4m_{2R}} \\ \omega_+ \mp (m_{1R} - m_{2R}) &= \frac{\mp\omega_-^2 \pm (\omega_+ \pm 2m_{2R})^2}{4m_{2R}}.\end{aligned}\quad (43)$$

Because $\alpha_{\pm h}$ and $\beta_{\pm h}$ are functions of a_{\pm} , b_{\pm} and c , (just as in the thin wall case (B6–B7)) there are no CP odd contributions in the mode mixing (Bogoliubov) coefficients (41). $\alpha_{\pm h}$ and $\beta_{\pm h}$ are indeed the usual Bogoliubov coefficients that transform an asymptotically early time vacuum state to a late time vacuum state. Hence $n_{\pm h} = |\beta_{\pm h}|^2$ is the particle number observed by a late time observer, in the late time state that evolves from the early time positive frequency vacuum state.

To make contact with the thin wall case (B6), we take the limit $\gamma \rightarrow \infty$ in (41) to get,

$$\beta_{\pm h} \xrightarrow{\gamma \rightarrow \infty} \mp \sqrt{\frac{[\omega_- \pm (m_{1R} + m_{2R})]}{\omega_+ \omega_- [\omega_+ \mp (m_{1R} - m_{2R})]}} \left[\frac{\omega_- - \omega_+}{2} \mp m_{2R} \right]. \quad (44)$$

It can be checked that Eq. (44) satisfies $\beta_{+h} = \beta_{-h}$. Moreover, since $\omega_- - \omega_+ - 2m_{2R} < 0$, the β_{+h} and β_{-h} are always positive. One can show that $\alpha_{\pm h}$ and $\beta_{\pm h}$ given in (41) obey $|\alpha_{\pm h}|^2 + |\beta_{\pm h}|^2 = 1$, as they should. This equality follows from,

$$\begin{aligned}|\alpha_{\pm h}|^2 &= \frac{\sinh\left(\frac{\pi[\omega_+ + \omega_- + 2m_{2R}]}{2\gamma}\right) \sinh\left(\frac{\pi[\omega_+ + \omega_- - 2m_{2R}]}{2\gamma}\right)}{\sinh\left(\frac{\pi\omega_+}{\gamma}\right) \sinh\left(\frac{\pi\omega_-}{\gamma}\right)} \\ n_{\pm h} = |\beta_{\pm h}|^2 &= \frac{\sinh\left(\frac{\pi[\omega_- - \omega_+ + 2m_{2R}]}{2\gamma}\right) \sinh\left(\frac{\pi[\omega_- - \omega_+ - 2m_{2R}]}{2\gamma}\right)}{\sinh\left(\frac{\pi\omega_+}{\gamma}\right) \sinh\left(\frac{\pi\omega_-}{\gamma}\right)},\end{aligned}\quad (45)$$

from which it also follows that $|\alpha_{\pm h}|^2 = 1 - |\beta_{\pm h}|^2$. Now, taking a thin wall limit $\gamma \rightarrow \infty$ in (45) yields

$$n_{\pm h} \xrightarrow{\gamma \rightarrow \infty} \frac{|m_- - m_+|^2 - (\omega_- - \omega_+)^2}{4\omega_- \omega_+}, \quad (46)$$

where we made use of Given that $4m_{2R}^2 = |m_- - m_+|^2$. This expression agrees with the thin wall particle number Eq. (B7) derived in appendix B.

It is interesting to note that, although particle number agrees, the Bogoliubov coefficient $\beta_{\pm h}$ in the thin wall limit (44) appears very different from the one derived explicitly for the thin wall (B6). For instance, the coefficients in (B6) are complex and depend explicitly on helicity, whereas the limiting coefficient (44) is real and helicity independent. A similar situation occurs for $\alpha_{\pm h}$, see (E8). The apparent discrepancy is caused by an overall phase factor by which the coefficients in the thin wall limit differ from those directly computed for the thin wall. This phase factor does not affect particle number and can be removed by a global rotation of the (anti)particle spinors. In appendix E we show explicitly how the kink wall case and thin wall case are connected.

The particle production can also be analyzed in the opposite limit, $\gamma \rightarrow 0$. In this thick wall regime particle production is exponentially suppressed as,

$$n_{\pm h} \xrightarrow{\gamma \rightarrow 0} \exp\left[-\frac{\pi(\omega_+ + \omega_- - 2m_{2R})}{\gamma}\right], \quad (47)$$

which is also what one expects. However, note that when $\pi(\omega_+ + \omega_- - 2m_{2R}) \lesssim \gamma$, the suppression is not large. This is demonstrated in figures 1 and 2, where the particle number is shown as a function of k for several different wall thicknesses. In figure 1 the mass parameters are $m_{1R} = m_{2R}$ and $m_I \ll m_{1R}, m_{2R}$. In this case CP violation is weak. For these mass parameters the thin wall particle number (46), represented by the dashed line, reaches the maximal particle number $n_{\pm h} = \frac{1}{2}$ as $k \rightarrow 0$. For thicker walls (decreasing γ) the particle number is exponentially suppressed with respect to the thin wall. For very small k the suppression is much smaller, since $\pi(\omega_+ + \omega_- - 2m_{2R})/\gamma \sim \sqrt{k^2 + m_I^2}/\gamma$.

In figure 2 the mass parameters are chosen such that $m_I, m_{1R} \ll m_{2R}$. In this case CP-violation is maximal for the thin wall in the limit $k \rightarrow 0$, see also (B9). The maximal particle number in this limit is 1, which indicates an inverse population. This inverse population, induced by large CP violation, is a novel result and, as far as we know,

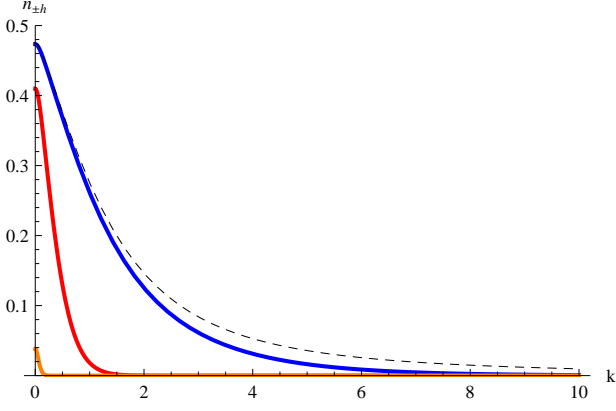


Figure 1: Plot of $n_{\pm h} = |\beta_{\pm h}|^2$ as function of k in units of m_{2R} . Parameters are $m_{1R} = m_{2R}$, $m_I = 0.1m_{2R}$. The dashed line is the thin wall solution of $n_{\pm h}$. The other (solid) lines show – from top to bottom – the particle numbers for $\gamma = 10m_{2R}$ (blue, dark), $\gamma = m_{2R}$ (red) and $\gamma = 0.1m_{2R}$ (orange, light). In general particle number is suppressed for decreasing γ (a thicker wall), but still a large particle number is reached when $k, m_I \ll m_{2R}$ and $m_{1R} - m_{2R} \simeq 0$.

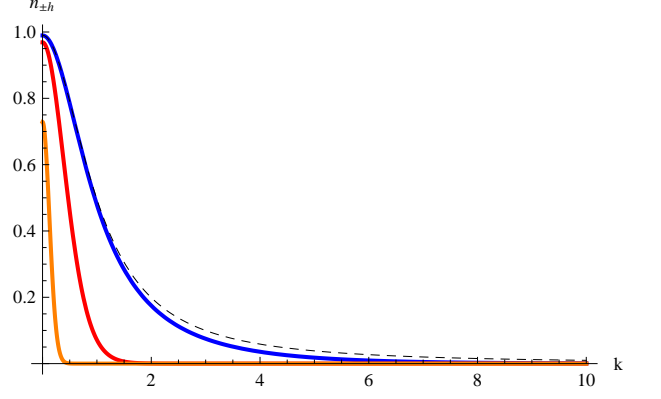


Figure 2: Plot of $n_{\pm h} = |\beta_{\pm h}|^2$ as function of k in units of m_{2R} . Parameters are $m_I = 0.1m_{2R}$, $m_{1R} = 0.1m_{2R}$. The dashed line is the thin wall solution of $n_{\pm h}$. The other (solid) lines show – from top to bottom – the particle numbers for $\gamma = 10m_{2R}$ (blue), $\gamma = m_{2R}$ (red) and $\gamma = 0.1m_{2R}$ (orange). Because $m_{1R} - m_{2R} < 0$, an inverse population is reached. The CP-violating phase is maximal because $m_+ \simeq -m_-$.

not noticed in literature before. For thicker walls the particle number is still suppressed, but much less than for the mass parameters in figure 1. In fact, for $m_{1R} = m_I = 0$ the particle number is unsuppressed in the limit $k \rightarrow 0$.

A large late time Bogoliubov particle number for a free fermionic system indicates large squeezing. It is interesting to see what effect such a large squeezing may have on the fermionic currents. In particular, we are interested in the CP-odd fermionic axial vector current that couples to sphalerons. The next section is devoted to computing these currents in the setting of a tanh-kink wall.

IV. THE CURRENTS AND CP VIOLATION

In this section we consider the evolution of the two point Wightman functions, defined as the expectation values [36, 59]

$$\imath S_{\alpha\beta}^{+-}(u, v) \equiv \imath S_{\alpha\beta}^{<}(u, v) = -\langle \hat{\psi}_\beta(v) \hat{\psi}_\alpha(u) \rangle; \quad \imath S_{\alpha\beta}^{-+}(u, v) \equiv \imath S_{\alpha\beta}^{>}(u, v) = \langle \hat{\psi}_\alpha(v) \hat{\psi}_\beta(v) \rangle, \quad (48)$$

and which satisfy the homogeneous Dirac equations (7)

$$(\imath \gamma^\mu \partial_\mu - m_R - \imath m_I \gamma^5) \imath S_{\alpha\beta}^{\pm\mp}(u, v) = 0. \quad (49)$$

For the problem at hand, when written in a Wigner mixed representation

$$\imath S_{\alpha\beta}^{\pm\mp}(u, v) = \int \frac{d^4 k}{(2\pi)^4} e^{\imath k \cdot (u-v)} \imath S_{\alpha\beta}^{\pm\mp}(k; x), \quad (x = (u+v)/2), \quad (50)$$

the fermionic Wightman function can be written in a helicity block-diagonal form

$$\imath S^{+-}(x; k) \equiv \imath S^{<} = \sum_{h=+,-} \imath S_h^{<}, \quad -\imath \gamma^0 S_h^{+-} = (\rho^a g_{ah}) \otimes \frac{1}{4} (1 + h \hat{k} \cdot \vec{\sigma}), \quad (51)$$

where σ^a, ρ^a ($a = 0, 1, 2, 3$) are the Pauli matrices and g_{ah} are the (off-shell) distribution functions measuring the vector, scalar, pseudo-scalar and pseudo-vector phase space densities of fermions, respectively. Their on-shell version

$$f_{ah} = \int \frac{dk_0}{2\pi} g_{ah}; \quad (a = 0, 1, 2, 3) \quad (52)$$

satisfy the following equations of motion [36, 59],

$$\begin{aligned}\dot{f}_{0h} &= 0 \\ \dot{f}_{1h} + 2hk f_{2h} - 2m_I f_{3h} &= 0 \\ \dot{f}_{2h} - 2hk f_{1h} + 2m_R f_{3h} &= 0 \\ \dot{f}_{3h} + 2m_I f_{1h} - 2m_R f_{2h} &= 0,\end{aligned}\tag{53}$$

where here $k \equiv \|\vec{k}\|$. To make the connection with section III and Appendix B, we note that one can express f_{ah} in terms of $u_{\pm h}$ or L_h and R_h as follows ²:

$$\begin{aligned}f_{0h} &= |u_{+h}|^2 + |u_{-h}|^2 = |R_h|^2 + |L_h|^2; & f_{3h} &= 2\Re[u_{+h}u_{-h}^*] = |L_h|^2 - |R_h|^2 \\ f_{1h} &= |u_{-h}|^2 - |u_{+h}|^2 = -2\Re[L_h R_h^*]; & f_{2h} &= 2\Im[u_{+h}u_{-h}^*] = -2\Im[L_h R_h^*].\end{aligned}\tag{54}$$

such that $f_{1h} + if_{2h} = -2L_h R_h^*$. From Eq. (A9) and (54) we immediately obtain that for $t \rightarrow -\infty$ ($z \rightarrow 0$),

$$f_{0h}^- = 1; \quad f_{1h}^- = -\frac{\Re[m_-]}{\omega_-}; \quad f_{2h}^- = -\frac{\Im[m_-]}{\omega_-}; \quad f_{3h}^- = -\frac{hk}{\omega_-},\tag{55}$$

where we took account of $u_{+h}u_{-h}^* = -(kh + im_I)/(2\omega_-)$, $z = \exp(2t/\tau)/[1 + \exp(2t/\tau)] \rightarrow \exp(2t/\tau)$ (as $t \rightarrow -\infty$) and of ${}_2F_1(a, b; c; 0) = 1$. Inserting Eqs. (55) into the particle number definition [59],

$$n_h(k, t) = \frac{m_R f_{1h} + m_I f_{2h} + hk f_{3h}}{2\omega} + \frac{1}{2},\tag{56}$$

yields that $n_h(k, t) = 0$ for $t \rightarrow -\infty$, as it should be since we have prepared the initial state to be in the pure free vacuum.

One can also consider the statistical particle number [62],

$$\bar{n}_{h\pm} = \frac{1}{2}f_{0h} \pm \frac{1}{2}\sqrt{f_{1h}^2 + f_{2h}^2 + f_{3h}^2}.\tag{57}$$

A statistical particle number is defined as the particle number associated with the basis in which the density operator is diagonal [62]. Statistical particle numbers can be used as a quantitative measure of state impurity, *i.e.* of how much a state deviates from a pure state. From previous work we have learned that the statistical particle number is constant in the absence of interactions. This can also be seen from the kinetic equations (53), which give

$$\frac{d}{dt}(f_{1h}^2 + f_{2h}^2 + f_{3h}^2) = 0.\tag{58}$$

Of course, when interactions are included, the righthand side of Eqs. (53) is in general nonzero. Here we consider a free Dirac equation (49), and therefore the statistical particle number should remain constant. Indeed, Eqs. (55) imply

$$f_{1h}^2 + f_{2h}^2 + f_{3h}^2 = [|u_{+h}|^2 + |u_{-h}|^2]^2 = 1,$$

such that the statistical particle numbers of a pure state are trivial,

$$\bar{n}_{\pm h} = \frac{1}{2}\left[f_{0h} \pm \sqrt{f_{1h}^2 + f_{2h}^2 + f_{3h}^2}\right] = \begin{cases} 1, \\ 0 \end{cases}.$$

Thus the statistical particle number is either 0 or 1, the latter corresponding to a fully occupied Dirac sea.

² Note that, due to difference in conventions, there are sign differences when compared with Ref. [59].

The exact solutions for the phase space densities f_{ah} as in Eq. (54) are complicated functions containing products of hypergeometric functions, which can be analyzed numerically. Analytically, we can study the behavior of f_{ah} 's in certain asymptotic limits. By making use of Eqs. (36-41), we get at asymptotically late times,

$$\begin{aligned}\tilde{u}_{+h} &\xrightarrow{t \rightarrow \infty} \alpha_{+h} \sqrt{\frac{\omega_+ + (m_{1R} - m_{2R})}{2\omega_+}} e^{-i\omega_+ t} + \beta_{+h} \sqrt{\frac{\omega_+ - (m_{1R} - m_{2R})}{2\omega_+}} e^{i\omega_+ t} \\ \tilde{u}_{-h} &\xrightarrow{t \rightarrow \infty} -\alpha_{-h} \frac{hk - im_I}{\sqrt{k^2 + m_I^2}} \sqrt{\frac{\omega_+ - (m_{1R} - m_{2R})}{2\omega_+}} e^{-i\omega_+ t} + \beta_{-h} \frac{hk - im_I}{\sqrt{k^2 + m_I^2}} \sqrt{\frac{\omega_+ + (m_{1R} - m_{2R})}{2\omega_+}} e^{i\omega_+ t}\end{aligned}\quad (59)$$

From these and Eqs. (39), (42) and (54) we easily obtain,

$$\begin{aligned}f_{0h}^+ &= 1 \\ f_{1h}^+ &= -\frac{m_R}{\omega_+} (1 - 2|\beta_{\pm}|^2) - \frac{2\sqrt{k^2 + m_I^2}}{\omega_+} [\Re[\alpha_{\pm h} \beta_{\pm h}^*] \cos(2\omega_+ t) + \Im[\alpha_{\pm h} \beta_{\pm h}^*] \sin(2\omega_+ t)] \\ f_{2h}^+ &= -\frac{m_I}{\omega_+} (1 - 2|\beta_{\pm}|^2) + \frac{2 \cos(2\omega_+ t)}{\omega_+ \sqrt{k^2 + m_I^2}} [\Re[\alpha_{\pm h} \beta_{\pm h}^*] m_I \Re[m_+] + \Im[\alpha_{\pm h} \beta_{\pm h}^*] hk \omega_+] \\ &\quad + \frac{2hk \sin(2\omega_+ t)}{\sqrt{k^2 + m_I^2}} [-\Re[\alpha_{\pm h} \beta_{\pm h}^*] + \Im[\alpha_{\pm h} \beta_{\pm h}^*]] \\ f_{3h}^+ &= -\frac{hk}{\omega_+} (1 - 2|\beta_{\pm}|^2) + \frac{2 \cos(2\omega_+ t)}{\omega_+ \sqrt{k^2 + m_I^2}} [\Re[\alpha_{\pm h} \beta_{\pm h}^*] hk \Re[m_+] - \Im[\alpha_{\pm h} \beta_{\pm h}^*] \omega_+ m_I] \\ &\quad + \frac{2 \sin(2\omega_+ t)}{\omega_+ \sqrt{k^2 + m_I^2}} [\Re[\alpha_{\pm h} \beta_{\pm h}^*] \omega_+ m_I + \Im[\alpha_{\pm h} \beta_{\pm h}^*] hk \Re[m_+]].\end{aligned}\quad (60)$$

Since we are primarily interested in the CP-violating axial vector currents, which can bias sphalerons, here we shall focus our attention primarily to f_{3h} . We can compute the CP-odd and CP-even axial vector phase space densities as follows,

$$\begin{aligned}\sum_{h=\pm} f_{3h}^+ &= \frac{4|\alpha_{\pm h}| |\beta_{\pm h}^*| m_I}{\sqrt{k^2 + m_I^2}} \sin(2\omega_+ t - \Delta\varphi) \\ \sum_{h=\pm} h f_{3h}^+ &= \frac{2k}{\omega_+} \left[-(1 - 2|\beta_{\pm}|^2) + \frac{2|\alpha_{\pm h}| |\beta_{\pm h}^*| m_{+R}}{\sqrt{k^2 + m_I^2}} \cos(2\omega_+ t - \Delta\varphi) \right],\end{aligned}\quad (61)$$

where

$$\Delta\varphi = \varphi_\alpha - \varphi_\beta, \quad (62)$$

φ_α and φ_β are the phases for $\alpha_{\pm h}$ and $\beta_{\pm h}$ in Eq. (41). In the thin wall limit $\gamma \rightarrow \infty$ the phases of $\alpha_{\pm h}$ and $\beta_{\pm h}$ are zero (see Eq. (E8)) and the CP-odd and -even phase space densities coincide with those in Eqs. (C11) (in the free vacuum). In the opposite 'thick wall' limit, $\gamma \rightarrow 0$,

$$\begin{aligned}\alpha_{\pm h} &\xrightarrow{\gamma \rightarrow 0} e^{i\varphi_\alpha} \\ \beta_{\pm h} &\xrightarrow{\gamma \rightarrow 0} \exp \left[-\frac{\pi(\omega_+ + \omega_- - 2m_{2R})}{2\gamma} \right] e^{i\varphi_\beta},\end{aligned}\quad (63)$$

with

$$\begin{aligned}\varphi_\alpha &\xrightarrow{\gamma \rightarrow 0} \frac{1}{\gamma} \left[-\omega_- \log(\omega_-) - \omega_+ \log(\omega_+) \right. \\ &\quad \left. + \left(\frac{\omega_- + \omega_+}{2} + m_{2R} \right) \log \left(\frac{\omega_- + \omega_+}{2} + m_{2R} \right) + \left(\frac{\omega_- + \omega_+}{2} - m_{2R} \right) \log \left(\frac{\omega_- + \omega_+}{2} - m_{2R} \right) \right] \\ \varphi_\beta &\xrightarrow{\gamma \rightarrow 0} \frac{1}{\gamma} \left[-\omega_- \log(\omega_-) + \omega_+ \log(\omega_+) \right. \\ &\quad \left. + \left(\frac{\omega_- - \omega_+}{2} + m_{2R} \right) \log \left(\frac{\omega_- - \omega_+}{2} + m_{2R} \right) - \left(\frac{-\omega_- + \omega_+}{2} + m_{2R} \right) \log \left(\frac{-\omega_- + \omega_+}{2} + m_{2R} \right) \right].\end{aligned}\quad (64)$$

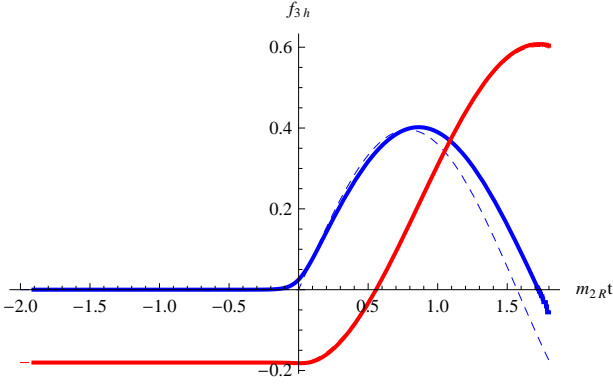


Figure 3: Odd (solid blue, darker) and even (solid red, lighter) part of the exact solution for f_{3h} for $\gamma = 10m_{2R}$. Parameters: $k = 0.1m_{2R}$, $\gamma = 10m_{2R}$, $m_I = 0.1m_{2R}$, $m_{1R} = 0.1m_{2R}$. The thin wall solutions (dashed) are constant for $t < 0$, and for $t > 0$ they oscillate with a frequency $2\omega_+$. The thin wall and exact result are nearly identical.

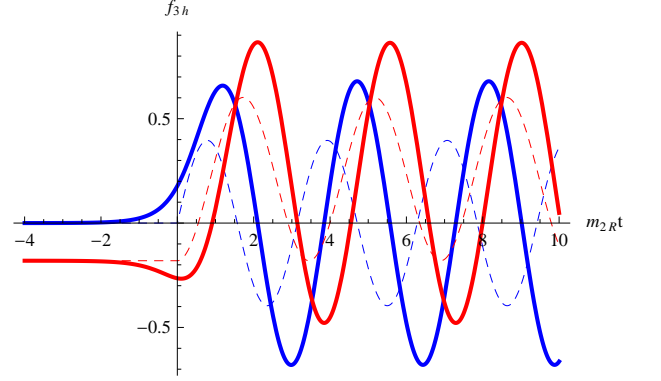


Figure 4: Odd (solid blue, dark) and even (solid red, lighter) part of the exact solution for f_{3h} for $\gamma = m_{2R}$. Parameters: $k = 0.1m_{2R}$, $\gamma = m_{2R}$, $m_I = 0.1m_{2R}$, $m_{1R} = 0.1m_{2R}$. For this wall of thickness $\gamma = m_{2R}$, the amplitude of the even and odd part of f_{3h} is slightly larger than the thin wall case (shown as dashed). Also, there is a moderate phase shift compared to the thin wall.

Thus, in this limit the phases φ_α and $-\varphi_\beta$ grow linearly with $1/\gamma$. In general, the oscillating CP-odd and CP-even phase space densities in the thick wall case therefore experience a phase shift compared to the thin wall, which can be large for small γ . Moreover, their amplitudes, which are proportional to $|\beta_{\pm h}|^2$ (see Eq. (61)), are generally suppressed compared to the thin wall limit. However, in the previous section we have demonstrated that the amplitude $|\beta_{\pm h}|$, or particle number $n_{h\pm}$, can become much less suppressed for a certain choice of parameters that leads to large squeezing, see figures 1–2. Due to this state large squeezing, the oscillations of the phase space densities are amplified.

Examples of this enhanced oscillatory behavior are depicted in figures 3–5. Here we show the exact solution for the odd and even part of f_{3h} using Eqs. (54) with solutions (34), and compare to the thin wall solutions (C11). The parameters are chosen such to generate large squeezing, thus $k \ll m_{2R}$ and the mass parameters are the same as those in figure 2. Close to the thin wall limit ($\gamma = 10m_{2R}$, figure 3) the exact solution for f_{3h} almost coincides with the thin wall result. For a thicker wall ($\gamma = m_{2R}$, figure 4) the amplitude of oscillations remains large and there is a modest phase shift compared to the thin wall. Finally, for a thick wall ($\gamma = .1m_{2R}$, figure 5) there is a large oscillatory enhancement and a large phase shift.

For thick walls a large squeezing can thus give a large enhancement of oscillations of the phase space density f_{3h} . However, due to the fact that phases of different modes \vec{k} differ, the oscillatory behavior may (partially) disappear when the corresponding currents are computed. These currents are related to the phase space densities f_{ah} as

$$j_{ah}(x) = \int \frac{d^3k}{(2\pi)^3} f_{ah}(\vec{k}; x), \quad (65)$$

where j_{0h} and j_{3h} denote the 0th components of the vector and axial vector current, respectively, and j_{1h} and j_{2h} are the scalar and pseudoscalar densities, respectively. In the following section we compare these integrated currents to those computed in a gradient approximation. First however, we shall show how to compute the currents for more general initial states.

A. Generalized initial state

So far the initial state has been taken in the free vacuum, such that $n_h(k, t) = 0$ for $t \rightarrow -\infty$. We can also consider the initial state to be thermally occupied, such that

$$n_h(k, t) \xrightarrow{t \rightarrow -\infty} \bar{n}_{th} = \frac{1}{e^{\beta\omega_-} + 1}. \quad (66)$$

The initial phase space densities that give this initial thermal state via Eq. (56) are now

$$f_{0h}^- = 1; \quad f_{1h}^- = -\frac{\Re[m_-]}{\omega_-}(1 - 2\bar{n}_{th}); \quad f_{2h}^- = -\frac{\Im[m_-]}{\omega_-}(1 - 2\bar{n}_{th}); \quad f_{3h}^- = -\frac{hk}{\omega_-}(1 - 2\bar{n}_{th}), \quad (67)$$

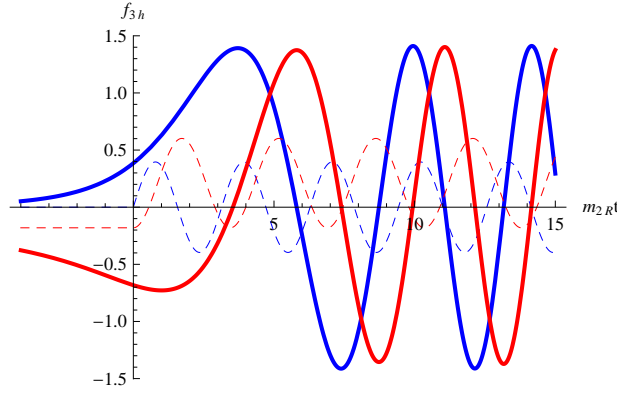


Figure 5: Odd (solid blue, dark) and even (solid red, lighter) part of the exact solution for f_{3h} for $\gamma = 0.1m_{2R}$ (solid line). Parameters: $k = 0.1m_{2R}$, $\gamma = 0.1m_{2R}$, $m_I = 0.1m_{2R}$, $m_{1R} = 0.1m_{2R}$. When CP-violation is maximal and squeezing is large (see figure 2) there is a large oscillatory enhancement for the odd and even phase space densities in the thick wall regime ($\gamma = 0.1m_{2R}$). Moreover, there is a large phase shift compared to the thin wall result (dashed).

Moreover, the statistical particle number (57) for $t \rightarrow -\infty$ is

$$\bar{n}_{h+} = 1 - \bar{n}_{th} \quad (68)$$

$$\bar{n}_{h-} = \bar{n}_{th}. \quad (69)$$

Using these relations the currents can also be written in terms of statistical particle number

$$f_{0h}^- = \bar{n}_{h+} + \bar{n}_{h-}; \quad f_{1h}^- = -\frac{\Re[m_-]}{\omega_-}(\bar{n}_{h+} - \bar{n}_{h-}); \quad f_{2h}^- = -\frac{\Im[m_-]}{\omega_-}(\bar{n}_{h+} - \bar{n}_{h-}); \quad f_{3h}^- = -\frac{hk}{\omega_-}(\bar{n}_{h+} - \bar{n}_{h-}). \quad (70)$$

Here, one can also consider general initial densities. In that case the statistical particle numbers \bar{n}_{h+} and \bar{n}_{h-} are both in the range $[0, 1]$ and conserved, but they are not necessarily related as in an initial state that is thermally occupied. The scalar density f_{0h} is in the range $[0, 2]$ and is still conserved. The initial state may be called an initial dense state, of which the thermal state (69) is a special case. One could further generalize the initial state to include initial squeezing, *etc.* For simplicity, we shall not consider here the more general cases.

As in the previous part we can compute the phase space densities f_{ah} for the kink wall, but now for general initial densities. Also here we can study the asymptotic late time behavior analytically. Again we are interested in the axial vector phase space density f_{3h} , which becomes in the asymptotic late time limit with general initial densities,

$$f_{3h}^+ = \left(-\frac{hk}{\omega_+}(1 - 2|\beta_{\pm}|^2) + \frac{\cos(2\omega_+t)}{2\omega_+\sqrt{k^2 + m_I^2}} [4\Re[\alpha_{\pm h}\beta_{\pm h}^*]m_{+R}hk - 4\Im[\alpha_{\pm h}\beta_{\pm h}^*]\omega_+m_I] \right. \\ \left. + \frac{\sin(2\omega_+t)}{2\omega_+\sqrt{k^2 + m_I^2}} [4\Re[\alpha_{\pm h}\beta_{\pm h}^*]\omega_+m_I + 4\Im[\alpha_{\pm h}\beta_{\pm h}^*]m_{+R}hk] \right) \times (\bar{n}_{h+} - \bar{n}_{h-}). \quad (71)$$

Thus, compared to Eq. (60), there is only an extra factor $\bar{n}_{h+} - \bar{n}_{h-}$ in f_{3h} , which appears similarly in f_{1h} and f_{2h} . We can now compute the CP-odd and CP-even phase space densities

$$\sum_{h=\pm} f_{3h}^+ = \left(\frac{4|\alpha_{\pm h}||\beta_{\pm h}^*|m_I}{\sqrt{k^2 + m_I^2}} \sin(2\omega_+t - \Delta\varphi) \right) \times (\bar{n}_{h+} - \bar{n}_{h-}) \\ \sum_{h=\pm} hf_{3h}^+ = \left(\frac{2k}{\omega_+} \left[-(1 - 2|\beta_{\pm}|^2) + \frac{2|\alpha_{\pm h}||\beta_{\pm h}^*|m_{+R}}{\sqrt{k^2 + m_I^2}} \cos(2\omega_+t - \Delta\varphi) \right] \right) \times (\bar{n}_{h+} - \bar{n}_{h-}), \quad (72)$$

where $\Delta\varphi$ is given in Eq. (62). For comparison, in appendix C we compute the fermionic phase space densities f_{ah} with a general initial state for a thin wall.

V. A COMPARISON WITH GRADIENT APPROXIMATION

In Refs. [48, 49] (see also Refs. [36, 37]) it was shown that the gradient approximation, when applied to the evolution equations for the Wightman functions, yields a semiclassical force which affects motion of particles in a plasma as a (planar) bubble wall of a first order electroweak transition sweeps through the electroweak plasma. The force is of the order \hbar , it is proportional to the spin orthogonal to the planar wall, and it has opposite sign for particles and antiparticles. Since up to now no analogous analysis has been performed for the time dependent case studied here (see however Refs. [59–61]), we shall present such an analysis here. The Dirac equation for a Wigner transformed (50) Wightman function $\mp i S^{\pm\mp}(u; v) = \langle \bar{\psi}(u) \psi(v) \rangle$ is of the form,

$$\left\{ \gamma^0 k_0 - \vec{\gamma} \cdot \vec{k} + \frac{i}{2} \gamma^0 \partial_t - [m_R(t) + i m_I(t) \gamma^5] \exp \left(- \frac{i}{2} \overleftarrow{\partial}_t \overrightarrow{\partial}_{k_0} \right) \right\} i S^{+-}(k; x) = 0, \quad (73)$$

where $x = (u + v)/2$ and k^μ is the Wigner momentum (the conjugate to $u - v$). One can show that the operator in Eq. (73) commutes with the helicity operator $\hat{H} = \hat{\vec{k}} \cdot \gamma^0 \vec{\gamma} \gamma^5$, implying that the Wightman function can be written as a sum of helicity diagonal 2×2 -blocks (51). With the *Ansatz* (51) one can construct non-local partial differential equations for the densities g_{ah} . The real and imaginary parts of these equations yield the constraint equations (CEs) and kinetic equations (KEs), respectively. The CEs and KEs can be subsequently solved in a gradient approximation. The technical details of these steps are in appendix F. Here we only present the main results. To first order in gradients, the CEs for g_{0h} and g_{3h} do not contain k_0 derivatives (here $\hbar = 1$):

$$(k_0^2 - |m|^2 - k^2) g_{0h} = 0 \quad (74)$$

$$\left(k_0^2 - |m|^2 - k^2 - h k \frac{|m|^2 \partial_t \theta}{k_0^2 - |m|^2} \right) g_{3h} = 0, \quad (75)$$

where the mass has been written as $m_R + i m_I = |m| e^{i\theta}$, and $k = \|\vec{k}\|$. General solutions to Eqs. (74–75) are of the form,

$$g_{0h} = \tilde{g}_{0h} 2\pi \delta(k_0^2 - |m|^2 - k^2), \quad g_{3h} = \tilde{g}_{3h} 2\pi \delta \left(k_0^2 - |m|^2 - k^2 - h \frac{|m|^2 \partial_t \theta}{k} \right). \quad (76)$$

Equations (74–76) reveal that at first order in derivatives (a) the vector density g_{0h} does not feel any effect of a changing background, while (b) the axial vector density g_{3h} lives on a shifted energy shell given by:

$$\omega_{3h} = \omega_0 + h \frac{|m|^2 \partial_t \theta}{2k\omega_0}; \quad \omega_0(t) = \sqrt{k^2 + |m(t)|^2}. \quad (77)$$

In analogy to the case of a planar wall, in which case the energy shift is, $\delta\omega_{\pm s} = \mp s |m|^2 (\partial_z \theta) / [2\omega_0 \sqrt{k_\perp^2 + |m|^2}]$, see Eq. (1) and Ref. [49], where \vec{k}_\perp is the momentum perpendicular to the wall and $s = \pm 1$ is the corresponding spin eigenvalue, Eq. (77) shows that the axial density g_{3h} lives on a shifted energy shell produced by the zero component of a fictitious ‘axial-vector field’ $h(|m|^2 \partial_t \theta) / (2k\omega_0)$. In this case however, the energy shift is proportional to helicity instead, it has identical sign for positive and negative frequency states and, as expected, it is proportional to a time derivative of the rate at which the mass argument $\theta = \text{Arg}[m]$ changes, which is a (good) measure of CP violation. Thus, just like in the case of a planar wall, the time dependent effect is a CP-violating shift, and thus can represent a source for baryogenesis.

In order to determine how this energy shift affects particle densities, we need to consider kinetic equations (to second order in gradients). These are derived in Eqs. (F22–F24) of appendix F. For g_{0h} and g_{3h} the KEs are

$$\partial_t g_{0h} + \frac{\partial_t |m|^2}{2} \partial_{k_0} \frac{g_{0h}}{k_0} = 0 \quad (78)$$

$$\partial_t g_{3h} + \frac{\partial_t |m|^2}{2k_0} \partial_{k_0} g_{3h} + h \frac{\partial_t (|m|^2 \partial_t \theta)}{2k k_0} \partial_{k_0} g_{3h} = 0. \quad (79)$$

Equation (78) teaches us that, as expected, the vector density g_{0h} does not feel any force at second order in gradients. The only effect that g_{0h} feels is a classical ‘force’, which is of first order in time derivative, and takes account of the energy non-conservation in a time dependent background $\omega_0(t)$. On the other hand, we see from (79) that the time dependent energy shift effect (77) produces as expected a second order semiclassical ‘force’ term in the kinetic equation for g_{3h} . These results are in accordance with what one would expect based on Eqs. (74–75). Just like in

the planar wall case, there is no second order $\partial_{k_0^2}$ term; only a term containing single k_0 derivative occurs in (79), justifying the name ‘force’. In fact, there is no force in (79). A better analogy is the Lorentz 4-force F^μ , where the 3-Lorentz force $\vec{F} = e(\vec{E} + \vec{v} \times \vec{B})$ constitutes the spatial part of F^μ , while the 0th component $F^0 = e\vec{v} \cdot \vec{E}$ yields the rate of energy loss in an electromagnetic field (which of course does not depend on the magnetic field \vec{B}). Similarly, in the above equations we can identify the rate of energy loss as the zeroth component of a 4-force,

$$F_h^0 = \frac{\partial_t |m|^2}{2\omega_{3h}} + h \frac{\partial_t (|m|^2 \partial_t \theta)}{2k\omega_0} = \partial_t \omega_{3h}(t), \quad (80)$$

where we projected $k_0 \rightarrow \pm\omega_{3h}$ on-shell in Eq. (79).

Now, the quantities f_{ah} considered in the rest of this paper are simply related to g_{ah} via the integral (52). In the light of Eq. (76) we see that the integral (52) just projects g_{ah} on the positive and negative frequency shells. Unless given differently by initial conditions, the positive and negative frequency projections are the same, and this fact does not change with time, because the semiclassical force is the same for both frequency shells. This is to be contrasted with the planar wall case, in which case the energy shift at the order \hbar has an opposite sign, see Eqs. (1–2). Of course, this simple picture is true only in the absence of interactions. When interactions are included, one expects off-shell effects in g_{ah} , and by performing the integral (52) one in general loses information.

Let us now integrate Eqs. (78) and (79) over k_0 . Integrating the first equation is easy, and yields a conservation of vector phase space density,

$$\partial_t f_{0h} = 0, \quad (81)$$

which is consistent with the more general result, which states that $f_{0h} = \text{const}$ in a free theory. Integrating Eq. (79) is more delicate, and yields

$$\partial_t f_{3h} + \left(\frac{\partial_t |m|^2}{2\omega_{3h}^2} + h \frac{\partial_t (|m|^2 \partial_t \theta)}{2k\omega_h^2} \right) f_{3h} = 0. \quad (82)$$

Since the expression in the parentheses is $\partial_t \ln(\omega_{3h})$, this equation can be simplified to,

$$\partial_t \ln(f_{3h}) = -\partial_t \ln(\omega_{3h}(t)), \quad (83)$$

and its solution is simply

$$f_{3h}(t) = \frac{\omega_3}{\omega_{3h}(t)} f_{3h}^-, \quad (84)$$

where ω_- is given in (31) and $f_{3h}^- = f_{3h}(t \rightarrow -\infty)$ (70). This means that, if one starts with $f_{3h} = -(kh/\omega_-) \times (\bar{n}_{h+} - \bar{n}_{h-})$ (see Eq. (70)), the gradient approximation yields,

$$f_{3h}(t) = -\frac{kh}{\omega_{3h}(t)} (\bar{n}_{h+} - \bar{n}_{h-}). \quad (85)$$

This result shows that gradient approximation captures the change in the frequency felt by particles, but does not see any quantum effects such as squeezing. Having a cursory look at figures 3–5 shows a striking feature: the large and oscillating contribution in the axial vector density is completely missed in gradient approximation. In afterthought, this should not come as surprise, since the oscillatory contributions to the densities come from state squeezing, which is a genuinely non-adiabatic quantum effect, and thus cannot be captured in a gradient (adiabatic) expansion. The question is whether this failure of gradient approximation means that an important effect is missed this way in regards to baryogenesis sources. The answer is not so simple as the plots in figures 3–5 suggest. Note that, when averaged over time, the oscillatory contributions disappear, and one is left with a mean effect. This mean effect is captured (to a certain extent) in gradient approximation (85). Indeed, Eq. (85) contains a CP-violating contribution, which is present during the time transient, and can be extracted from the CP-odd part of Eq. (85),

$$\sum_{h=\pm} f_{3h}(t) = \frac{|m|^2 \partial_t \theta}{\omega_0^3} (1 - 2\bar{n}_{\text{th}}), \quad (86)$$

where for simplicity we took an initial thermal state, $\bar{n}_{h+} - \bar{n}_{h-} \rightarrow 1 - 2\bar{n}_{\text{th}}$, $\bar{n}_{\text{th}} = 1/[\exp(\beta\omega_-) + 1]$.

In order to compare the CP-odd axial density in the gradient approximation (86) to the exact results (see figures 3–5), we integrate the phase space densities over the momenta (65) and sum over the helicities, which gives the CP

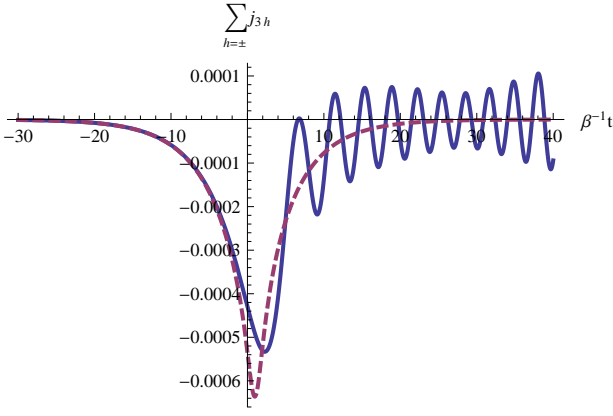


Figure 6: Difference between the finite temperature and zero temperature CP-odd axial vector current for the exact solution (blue, solid) and gradient approximation (red, dashed) for a thick wall with $\gamma = 0.1\beta^{-1}$. The mass parameters are: $m_I = 0.1\beta^{-1}$, $m_{1R} = 0.1\beta^{-1}$, $m_{2R} = \beta^{-1}$.

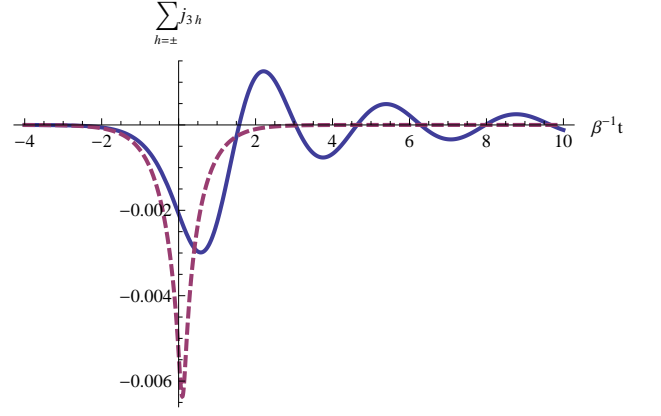


Figure 7: Difference between the finite temperature and zero temperature CP odd axial vector current for the exact solution (blue, solid) and gradient approximation (red, dashed) for a wall with $\gamma = \beta^{-1}$. The mass parameters are: $m_I = 0.1\beta^{-1}$, $m_{1R} = 0.1\beta^{-1}$, $m_{2R} = \beta^{-1}$.

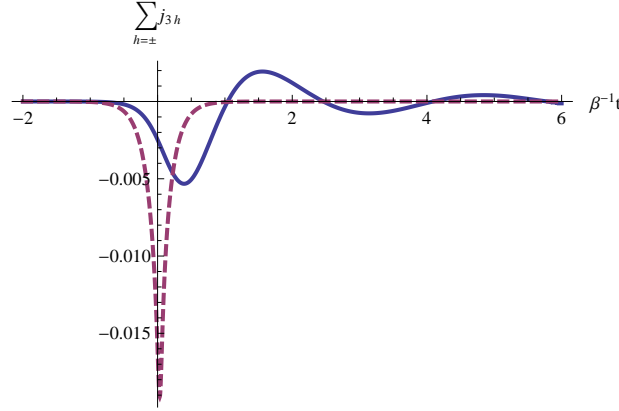


Figure 8: Difference between the finite temperature and zero temperature CP odd axial vector current for the exact solution (blue, solid) and gradient approximation (red, dashed) for a wall with $\gamma = 3\beta^{-1}$. The mass parameters are: $m_I = 0.1\beta^{-1}$, $m_{1R} = 0.1\beta^{-1}$, $m_{2R} = \beta^{-1}$.

odd current $\sum_{h=\pm} j_{3h}$. The zero temperature part of the current however diverges as $k \rightarrow \infty$. Therefore we only compare the finite temperature parts of the integrated f_{3h} 's, that is, only the part that is Boltzmann suppressed. Technically we compute $\sum_{h=\pm} [j_{3h}(\beta) - j_{3h}(\beta \rightarrow \infty)]$, the difference between the CP-odd axial vector current at finite temperature and the current at zero temperature.

In figures 6, 7 and 8 we show the finite part of the CP-odd current for the gradient expansion and for the exact solution, for a thick wall with $\gamma = 0.1\beta^{-1}$, a wall of thickness $\gamma = \beta^{-1}$, and a thin wall with $\gamma = 3\beta^{-1}$ respectively.³ The mass parameters are chosen such that there is a large state squeezing. The gradient expansion captures quite well the main trend, but misses the oscillations at later times. It is intriguing that already for the wall with $\gamma = \beta^{-1}$, the exact solution for the current starts to look quite different from the current in the gradient approximation. For the thin wall in Fig. 8 the difference is even more significant. It would be interesting to explore in more detail the

³ Note that, based on Eqs. (3) and (4) in the introduction, modes of both the thin and thick wall regime contribute to the integrated density, *i.e.* to the current. The question is therefore, whether the currents in Figs. 6–8 are dominated by modes that satisfy the thick wall condition, or by thin wall modes. Roughly speaking, for $\beta\gamma \ll 1$ the current is largely dominated by thick wall modes, whereas for $\beta\gamma \gg 1$ modes that satisfy the thin wall condition contribute mostly to the current.

CP-violating current in the thinner wall regime. Needless to say, in order to make a definite statement about the validity of gradient approximation, one needs to perform a more detailed analysis which includes scatterings coming from quantum loop effects.

VI. CONCLUSIONS AND DISCUSSION

In this work we derive an exact solution of the Dirac equation for fermions with a time dependent mass, generated by a scalar Higgs condensate. We assume that the mass has a tanh time dependence, which represents a quite realistic model for phase interface (bubble wall) at a first order phase transition in the early Universe setting. Moreover, the mass is complex with a phase changing in time, which can be a source for CP violation. We have studied this CP violation by looking at the CP-odd part of the axial vector current, since that current biases sphaleron transitions.

As already emphasized in the introduction the division between "thin wall" and "thick wall" cases depends on the relevant momenta, and both cases are present in a typical (say thermal) distribution. For large state squeezing, *i.e.* a large late time Bogoliubov particle production, the axial vector phase space density for a thick wall experiences a large oscillatory enhancement and phase shift with respect to the thin wall case. This non-adiabatic behavior cannot be captured by the gradient approximation. However, the mean effect for the axial vector current, which is obtained from the phase space density after summing the momenta, is described reasonably well in gradient approximation. Still, the exact solution for the axial vector current shows that the difference for thinner walls can be quite significant. This invites for a more detailed quantitative study of baryogenesis sources in the thin wall regime.

Extensions to our work can be foreseen. First of all, instead of a time dependent mass, our analysis can be generalized to a planar wall case, in which the mass is dependent on one spatial coordinate. This extension is in principle straightforward, and has been considered for the CP-conserving case in Ref. [56, 57], except that we intend to work now with full inclusion of a CP-violating mass. Moreover, whereas we consider one non-interacting fermionic species, one could also study multiple flavors. In that case, there is an additional CP-violating source in the flavor mixing mass matrix. It would be interesting to see what is the dominant source of CP violation depending on wall thickness. Finally, we did not include other effects such as plasma scatterings, and it would be worthwhile to explore how these affect the analytical results in this work.

VII. ACKNOWLEDGEMENTS

We thank Kimmo Kainulainen and Pyry Rahkila for useful discussions concerning the gradient expansion. TP and JW were in part supported by the Dutch Foundation for 'Fundamenteel Onderzoek der Materie' (FOM) under the program "Theoretical particle physics in the era of the LHC", program number FP 104.

Appendix A: Mode functions for a constant mass

In this appendix we construct the fundamental solutions of Eqs. (17)–(18) for a constant mass. In appendix B we treat the thin wall case.

When the mass is constant, the general solution of Eqs. (17–18) (see also Eqs. (7–16)) can be written as plane waves,

$$\begin{aligned} L_h &= A_h e^{-i\omega t} + B_h e^{i\omega t}; & R_h &= C_h e^{-i\omega t} + D_h e^{i\omega t} \\ \bar{L}_h &= \bar{A}_h e^{i\omega t} + \bar{B}_h e^{-i\omega t}; & \bar{R}_h &= \bar{C}_h e^{i\omega t} + \bar{D}_h e^{-i\omega t}, \end{aligned} \quad (\text{A1})$$

where $A_h, B_h, C_h, D_h, \bar{A}_h, \bar{B}_h, \bar{C}_h$ and \bar{D}_h are constants. The first order equations (17–18) tell us that C_h and D_h can be expressed in terms of A_h and B_h :

$$C_h = \frac{m^*}{\omega - hk} A_h = \frac{\omega + hk}{m} A_h = \frac{m^*}{|m|} \sqrt{\frac{\omega + hk}{\omega - hk}} A_h; \quad D_h = -\frac{m^*}{\omega + hk} B_h = -\frac{\omega - hk}{m} B_h = -\frac{m^*}{|m|} \sqrt{\frac{\omega - hk}{\omega + hk}} B_h. \quad (\text{A2})$$

Notice that these equations also imply an on-shell condition, $\omega^2 = k^2 + |m|^2$. Analogous relations hold for the barred constants,

$$\bar{C}_h = -\frac{m^*}{\omega - hk} \bar{A}_h = -\frac{\omega + hk}{m} \bar{A}_h = -\frac{m^*}{|m|} \sqrt{\frac{\omega + hk}{\omega - hk}} \bar{A}_h; \quad \bar{D}_h = \frac{m^*}{\omega + hk} \bar{B}_h = \frac{\omega - hk}{m} \bar{B}_h = \frac{m^*}{|m|} \sqrt{\frac{\omega - hk}{\omega + hk}} \bar{B}_h. \quad (\text{A3})$$

These constants can be further constrained by imposing the vector current conservation law, which in the absence of flavour mixing becomes particularly simple, $\partial_t j^0(x) = 0$, or equivalently $j^0(x) = \langle \psi^\dagger(x) \psi(x) \rangle = \text{const.}$ In order to fix the constant, notice that

$$\langle \hat{\psi}_\beta^\dagger(\vec{x}, t) \hat{\psi}_\alpha(\vec{x}', t) \rangle = \frac{1}{2} \langle \{ \hat{\psi}_\beta^\dagger(\vec{x}, t), \hat{\psi}_\alpha(\vec{x}', t) \} \rangle + \frac{1}{2} \langle [\hat{\psi}_\beta^\dagger(\vec{x}, t), \hat{\psi}_\alpha(\vec{x}', t)] \rangle = \frac{1}{2} \delta_{\alpha\beta} \delta^3(\vec{x} - \vec{x}') - F_{\alpha\beta}(\vec{x}, t; \vec{x}', t), \quad (\text{A4})$$

where $F_{\alpha\beta}(\vec{x}, t; \vec{x}', t)$ the Hadamard (statistical) Green function, which in the free space vanishes⁴. When written in momentum space

$$\hat{\psi}(\vec{x}, t) = \int \frac{d^3 k}{(2\pi)^3} e^{i\vec{k} \cdot \vec{x}} \hat{\psi}(\vec{k}, t) \quad (\text{A5})$$

Eq. (A4) becomes,

$$\langle \hat{\psi}_\beta^\dagger(\vec{k}, t) \hat{\psi}_\alpha(\vec{k}, t) \rangle = \frac{1}{2} \langle \{ \hat{\psi}_\beta^\dagger(\vec{k}, t), \hat{\psi}_\alpha(\vec{k}, t) \} \rangle + \frac{1}{2} \langle [\hat{\psi}_\beta^\dagger(\vec{k}, t), \hat{\psi}_\alpha(\vec{k}, t)] \rangle = \frac{1}{2} \delta_{\alpha\beta}, \quad (\text{A6})$$

where the expectation value was taken with respect to the vacuum state $|\Omega\rangle$, in which case $F = 0$. Similarly we have,

$$\langle \hat{\psi}_\alpha(\vec{k}, t) \hat{\psi}_\beta^\dagger(\vec{k}, t) \rangle = \frac{1}{2} \delta_{\alpha\beta} + F_{\alpha\beta}(k, t; t) \rightarrow \frac{1}{2} \delta_{\alpha\beta}. \quad (\text{A7})$$

Taking a trace of (A6–A7) one finds,

$$\sum_h (|\bar{L}_h|^2 + |\bar{R}_h|^2) = \frac{1}{2} \text{Tr}[\delta_{\alpha\beta}] = 2, \quad \sum_h (|L_h|^2 + |R_h|^2) = \frac{1}{2} \text{Tr}[\delta_{\alpha\beta}] = 2,$$

which implies:

$$|\bar{L}_h|^2 + |\bar{R}_h|^2 = 1 = |L_h|^2 + |R_h|^2, \quad (\text{A8})$$

where we assumed that the vacuum state normalization is independent of helicity. Moreover, since $\xi_h^\dagger \cdot \xi_{h'} = \delta_{hh'}$, Eq. (A8) agrees with (13). Together with (A2–A3) the condition (A8) allows one to completely specify the vacuum fermionic mode functions for constant mass (up to an overall phase),

$$\begin{aligned} L_h(k, t) &= \sqrt{\frac{\omega - hk}{2\omega}} e^{-i\omega t}, & R_h(k, t) &= \sqrt{\frac{\omega + hk}{2\omega}} \frac{m^*}{|m|} e^{-i\omega t} \\ \bar{L}_h(k, t) &= \sqrt{\frac{\omega - hk}{2\omega}} e^{i\omega t}, & \bar{R}_h(k, t) &= -\sqrt{\frac{\omega + hk}{2\omega}} \frac{m^*}{|m|} e^{i\omega t} \end{aligned} \quad (\text{A9})$$

Notice that these solutions satisfy the mode normalization conditions (A8). Moreover, (when summed over h) they also satisfy the (stronger) consistency condition (11). The only remaining conditions to check are the mode orthogonality conditions (12). They imply,

$$\bar{L}_h^* R_h + \bar{R}_h^* L_h = 0$$

For the solutions above, this implies,

$$e^{-2i\omega t} \frac{1}{2\omega} [m^* - m] = 0,$$

which can be only satisfied if $\Im[m] = 0$. There is no problem when m is time independent. In this case one can perform a global rotations on spinors that removes the imaginary part of the mass,

$$\psi \rightarrow e^{-i\theta\gamma^5} \psi = [\cos(\theta) - i\sin(\theta)\gamma^5] \psi, \quad \bar{\psi} \rightarrow \bar{\psi} e^{-i\theta\gamma^5} = \bar{\psi} [\cos(\theta) - i\sin(\theta)\gamma^5],$$

⁴ This definition of the Hadamard function differs by a constant from the definition used in *e.g.* Ref. [62], which is due to the normal ordering of the creation and annihilation operators, assumed in the construction of the density operator in Ref. [62].

where

$$\tan(2\theta) = \frac{m_I}{m_R}, \quad \cos(2\theta) = \frac{m_R}{|m|}, \quad \sin(2\theta) = \frac{m_I}{|m|},$$

with which

$$-m\bar{\psi}\psi_R - m^*\bar{\psi}\psi_L = -m_R\bar{\psi}\psi - im_I\bar{\psi}\gamma^5\psi \rightarrow -|m|\bar{\psi}\psi.$$

Of course, this rotation is global, and works only if m is time independent. Here we are interested in a time dependent problem, and hence the mode functions are not orthogonal as in (12). Is this a problem? Not necessarily. What is important is that the mode functions span the whole Hilbert space. The most important condition that must be satisfied is in the end Eq. (13). Note also that

$$\bar{\chi}_h(\vec{k}, t) \cdot \chi_h(\vec{k}, t) = \frac{m_R}{\omega} = -\bar{\nu}_h(\vec{k}, t) \cdot \nu_h(\vec{k}, t). \quad (\text{A10})$$

Appendix B: Mode functions for a step fermion mass

We shall now assume that the mass takes a simple form, such that it exhibits a sudden jump at $t = 0$:

$$m(t) = m_- \Theta(-t) + m_+ \Theta(t) \quad (\text{B1})$$

where m_- and m_+ are (in general complex) constant masses at negative and positive times, respectively. This is what we refer to as the thin wall mass profile. One can easily convince oneself that a constant $U(1)$ rotation of the left- and right-handed spinors in (5) can remove a jump in the *e.g.* imaginary part of the mass. After performing such a rotation the mass can be written as $m_{\pm} = |m_{\pm}| \exp[i(\phi_{\pm} + \chi)]$, where χ is the relative phase between left- and right-handed spinors. One should then solve $|m_+| \sin(\phi_+ + \chi) = |m_-| \sin(\phi_- + \chi)$ for χ .⁵ Therefore, without any loss of generality, one can assume that $\Im[m(t)] = \text{const.}$, or equivalently, $\Im[m_+] = \Im[m_-]$. This will be important for decoupling of the equations for $u_{\pm h}$ defined below (see also Eq. (25)).

For the problem at hand with $m(t)$ given in (B1), we can make the following *Ansätze* for the mode functions (*cf.* Eqs. (A9)),

$$\begin{aligned} L_h(k, t) &= \theta(-t)L_h^- + \theta(t)L_h^+ \\ R_h(k, t) &= \theta(-t)R_h^- + \theta(t)R_h^+ \\ \bar{L}_h(k, t) &= \theta(-t)\bar{L}_h^- + \theta(t)\bar{L}_h^+ \\ \bar{R}_h(k, t) &= \theta(-t)\bar{R}_h^- + \theta(t)\bar{R}_h^+, \end{aligned} \quad (\text{B2})$$

where the solutions for $t < 0$ are vacuum mode functions derived in (A9),

$$L_h^- = \sqrt{\frac{\omega_- - hk}{2\omega_-}} e^{-i\omega_- t}; \quad R_h^- = \sqrt{\frac{\omega_- + hk}{2\omega_-}} \frac{m_-^*}{|m_-|} e^{-i\omega_- t}; \quad \bar{L}_h^- = \sqrt{\frac{\omega_- - hk}{2\omega_-}} e^{i\omega_- t}; \quad \bar{R}_h^- = -\sqrt{\frac{\omega_- + hk}{2\omega_-}} \frac{m_-}{|m_-|} e^{i\omega_- t}. \quad (\text{B3})$$

The solutions for $t > 0$ can now be written as a linear combination of the normalized positive and negative frequency

⁵ The exact solution gives

$$\chi = \arctan\left(-\frac{m_{-I} - m_{+I}}{m_{-R} - m_{+R}}\right)$$

solutions

$$\begin{aligned}
L_h^+ &\equiv L_h(t > 0) = \alpha_h^+ \sqrt{\frac{\omega_+ - hk}{2\omega_+}} e^{-i\omega_+ t} + \beta_h^+ \sqrt{\frac{\omega_+ + hk}{2\omega_+}} e^{i\omega_+ t} \\
R_h^+ &\equiv R_h(t > 0) = \alpha_h^+ \sqrt{\frac{\omega_+ + hk}{2\omega_+}} \frac{m_+^*}{|m_+|} e^{-i\omega_+ t} - \beta_h^+ \sqrt{\frac{\omega_+ - hk}{2\omega_+}} \frac{m_+^*}{|m_+|} e^{i\omega_+ t} \\
\bar{L}_h^+ &\equiv \bar{L}_h(t > 0) = \bar{\alpha}_h^+ \sqrt{\frac{\omega_+ - hk}{2\omega_+}} e^{i\omega_+ t} + \bar{\beta}_h^+ \sqrt{\frac{\omega_+ + hk}{2\omega_+}} e^{-i\omega_+ t} \\
\bar{R}_h^+ &\equiv \bar{R}_h(t > 0) = -\bar{\alpha}_h^+ \sqrt{\frac{\omega_+ + hk}{2\omega_+}} \frac{m_+^*}{|m_+|} e^{i\omega_+ t} + \bar{\beta}_h^+ \sqrt{\frac{\omega_+ - hk}{2\omega_+}} \frac{m_+^*}{|m_+|} e^{-i\omega_+ t},
\end{aligned} \tag{B4}$$

where

$$\omega_{\pm} = \sqrt{k^2 + |m_{\pm}|^2},$$

and the solutions multiplying β_h^+ and $\bar{\beta}_h^+$ are the normalized negative frequency solutions of Eqs. (17)–(18). The four Bogoliubov coefficients in (B2) are determined by the matching conditions. Eqs. (17–18) together with the structure of the mass term (B1) tell us that the mode functions must be continuous at $t = 0$, which implies the following four matching conditions

$$L_h(t = 0-) = L_h(t = 0+); \quad R_h(t = 0-) = R_h(t = 0+); \quad \bar{L}_h(t = 0-) = \bar{L}_h(t = 0+); \quad \bar{R}_h(t = 0-) = \bar{R}_h(t = 0+). \tag{B5}$$

These conditions imply for the Bogoliubov coefficients in the solutions for L_h and R_h in Eq. (B2):

$$\begin{aligned}
\alpha_h^+ = \bar{\alpha}_h^+ &= \frac{|m_+|}{2\sqrt{\omega_+ \omega_-}} \left(\sqrt{\frac{\omega_- - hk}{\omega_+ + hk}} + \frac{m_-^*}{m_+^*} \sqrt{\frac{\omega_+ + hk}{\omega_- - hk}} \right) \\
\beta_h^+ = \bar{\beta}_h^+ &= \frac{|m_+|}{2\sqrt{\omega_+ \omega_-}} \left(\sqrt{\frac{\omega_- - hk}{\omega_+ - hk}} - \frac{m_-^*}{m_+^*} \sqrt{\frac{\omega_+ - hk}{\omega_- - hk}} \right).
\end{aligned} \tag{B6}$$

By observing that $|\alpha_h^+|^2 + |\beta_h^+|^2 = 1$ one can easily check that these conditions satisfy the correct normalization condition (A8).

To summarize, our simple calculation shows that, as a consequence of a sudden mass change (at $t = 0$), the number of fermions (of each helicity h) produced is

$$n_h = |\beta_h^+|^2 = \frac{|m_+ - m_-|^2 - (\omega_+ - \omega_-)^2}{4\omega_+ \omega_-} = \frac{1}{2} - \frac{k^2 + \Re[m_+ m_-^*]}{2\omega_+ \omega_-} \tag{B7}$$

which is helicity independent and, in general, does not vanish. One can show that n_h in (B7) satisfies, $0 \leq n_h(k) \leq 1$ for arbitrary \vec{k} , m_+ and m_- , which is a nontrivial check of the correctness of (B7). Note finally that, when $k = 0$,

$$n_h = \frac{1}{2} \left[1 - \frac{\Re[m_+ m_-^*]}{|m_+| |m_-|} \right]. \tag{B8}$$

This last result nicely illustrates the dependence of particle production on the complex phase of the mass. Let us denote $m_{\pm} = |m_{\pm}| e^{i\theta_{\pm}}$. Then

$$n_h = \frac{1}{2} [1 - \cos(\theta_+ - \theta_-)] = \sin^2 \left(\frac{\theta_+ - \theta_-}{2} \right), \tag{B9}$$

which shows that n_h varies between 0 and 1, as it should. There is no particle production when $\theta_+ - \theta_- = 2\pi n$ ($n \in \mathbb{Z}$), in which case there is no CP violation. On the other hand, when $k = 0$ particle production maximizes for $\theta_+ - \theta_- = \pi(2n + 1)$ ($n \in \mathbb{Z}$), in which case CP violation is maximal. This is in accordance with the results of finite wall thickness (45–47), shown in figures 1–2.

Appendix C: Two point functions for a step fermion mass

In this section we consider the evolution of the two point functions with a Heaviside step function mass (B1). Here we heavily use Ref. [59]. By making use of (54) we can find the phase space densities for the thin wall mass profile. For $t < 0$, the phase space densities are given in Eq. (55). Together with Eqs. (B4), Eqs. (B2) can be used to compute f_{ah} for $t > 0$.

Instead of calculating the f_{ah} by using the explicit expressions for the mode functions, we can also derive the phase space densities from the kinetic equations (53). We consider a generalized initial state, for which the f_{ah} for $t < 0$ are given by Eq. (70). Next we solve the f_{ah} for $t > 0$ from the kinetic equations (53). In order to do so, note first that Eqs. (B4) and (54) imply that the general form of the solutions for $t > 0$ is,

$$f_{ah}^+ = \alpha_{ah} \cos(2\omega_+ t) + \beta_{ah} \sin(2\omega_+ t) + \gamma_{ah} \quad (a = 0, 1, 2, 3), \quad (C1)$$

where α_{ah} , β_{ah} and γ_{ah} are constants that can be determined from the matching conditions at $t = 0$. Although m experiences a finite jump at $t = 0$, the structure of the equations of motion (53) implies that all of f_{ah} must be continuous at $t = 0$:

$$f_{ah}^-(k, t = 0) = f_{ah}^+(k, t = 0). \quad (C2)$$

The first equation in (53) tells us that the vector particle density f_{0h} cannot depend on time, *i.e.* that $\alpha_{0h} = \beta_{0h} = 0$, and we have:

$$f_{0h}^+ = \bar{n}_{h+} + \bar{n}_{h-}. \quad (C3)$$

The other three equations in (53) give nine conditions among the parameters $\{\alpha_{ih}, \beta_{ih}, \gamma_{ih}\}$ ($i = 1, 2, 3$). These conditions represent a highly degenerate system, such that the following independent conditions remain:

$$m_R^+ \alpha_{1h} + m_I^+ \alpha_{2h} + hk \alpha_{3h} = 0; \quad m_R^+ \beta_{1h} + m_I^+ \beta_{2h} + hk \beta_{3h} = 0; \quad \gamma_{2h} = \frac{m_I^+}{m_R^+} \gamma_{1h}; \quad \gamma_{3h} = \frac{hk}{m_R^+} \gamma_{1h}. \quad (C4)$$

In addition, β_{ih} are related to α_{ih} as follows:

$$\beta_{1h} = -\frac{hk}{\omega_+} \alpha_{2h} + \frac{m_I^+}{\omega_+} \alpha_{3h}; \quad \beta_{2h} = \frac{hk}{\omega_+} \alpha_{1h} - \frac{m_R^+}{\omega_+} \alpha_{3h}; \quad \beta_{3h} = -\frac{m_I^+}{\omega_+} \alpha_{1h} + \frac{m_R^+}{\omega_+} \alpha_{2h}. \quad (C5)$$

Furthermore, the matching conditions (C2) result in:

$$-\frac{m_R^-}{\omega_-} (\bar{n}_{h+} - \bar{n}_{h-}) = \alpha_{1h} + \gamma_{1h}; \quad -\frac{m_I^-}{\omega_-} (\bar{n}_{h+} - \bar{n}_{h-}) = \alpha_{2h} + \gamma_{2h}; \quad -\frac{hk}{\omega_-} (\bar{n}_{h+} - \bar{n}_{h-}) = \alpha_{3h} + \gamma_{3h}, \quad (C6)$$

which, together with Eqs. (C4–C5) completely specify f_{ih} . When the solutions for the α_{ih} , β_{ih} and γ_{ih} are inserted into the general form (C1), we find

$$f_{1h}^+ = \left(\left[-\frac{m_R^-}{\omega_-} + \frac{m_R^+}{\omega_+} \frac{k^2 + \Re[m_+ m_-^*]}{\omega_+ \omega_-} \right] \cos(2\omega_+ t) + \left[\frac{hk}{\omega_- \omega_+} (m_I^- - m_I^+) \right] \sin(2\omega_+ t) - \frac{m_R^+}{\omega_+} \frac{k^2 + \Re[m_+ m_-^*]}{\omega_+ \omega_-} \right) \times (\bar{n}_{h+} - \bar{n}_{h-}) \quad (C7)$$

$$f_{2h}^+ = \left(\left[-\frac{m_I^-}{\omega_-} + \frac{m_I^+}{\omega_+} \frac{k^2 + \Re[m_+ m_-^*]}{\omega_+ \omega_-} \right] \cos(2\omega_+ t) - \left[\frac{hk}{\omega_- \omega_+} (m_R^- - m_R^+) \right] \sin(2\omega_+ t) - \frac{m_I^+}{\omega_+} \frac{k^2 + \Re[m_+ m_-^*]}{\omega_+ \omega_-} \right) \times (\bar{n}_{h+} - \bar{n}_{h-}) \quad (C8)$$

$$f_{3h}^+ = \left(\left[-\frac{hk}{\omega_-} + \frac{hk}{\omega_+} \frac{k^2 + \Re[m_+ m_-^*]}{\omega_+ \omega_-} \right] \cos(2\omega_+ t) + \frac{\Im[m_+ m_-^*]}{\omega_+ \omega_-} \sin(2\omega_+ t) - \frac{hk}{\omega_+} \frac{k^2 + \Re[m_+ m_-^*]}{\omega_+ \omega_-} \right) \times (\bar{n}_{h+} - \bar{n}_{h-}), \quad (C9)$$

It can be checked that the same phase space densities are obtained by inserting the mode functions for $t > 0$ Eqs. (B4) in the definitions for f_{ah} Eqs. (B2).

The final produced particle number (56) is

$$n_h = \frac{1}{2} - \left(\frac{k^2 + \Re[m_+ m_-^*]}{2\omega_+ \omega_-} \right) \times (\bar{n}_{h+} - \bar{n}_{h-}). \quad (C10)$$

For the free vacuum, where $\bar{n}_{h+} = 1$ and $\bar{n}_{h-} = 0$, this indeed reduces to the result computed before, Eq. (B7). The thermal limit is obtained when $\bar{n}_{h+} - \bar{n}_{h-} \rightarrow 1 - 2\bar{n}_{\text{th}}$, $\bar{n}_{\text{th}} = 1/(e^{\beta\omega_+} + 1)$.

To get the CP-violating density, which is of relevance for baryogenesis, we finally need to sum the axial density f_{3h} over $h = \pm$,

$$\begin{aligned} \sum_{h=\pm} h f_{3h} &= \left(-\frac{2k}{\omega_+} \frac{k^2 + \Re[m_+ m_-^*]}{\omega_+ \omega_-} + \left[-\frac{2k}{\omega_-} + \frac{2k}{\omega_+} \frac{k^2 + \Re[m_+ m_-^*]}{\omega_+ \omega_-} \right] \cos(2\omega_+ t) \right) \times (\bar{n}_{h+} - \bar{n}_{h-}) \\ \sum_{h=\pm} f_{3h} &= \frac{2|m_+||m_-|\sin(\theta_+ - \theta_-)}{\omega_+ \omega_-} \sin(2\omega_+ t) \times (\bar{n}_{h+} - \bar{n}_{h-}), \end{aligned} \quad (\text{C11})$$

where in the last equality we used, $m_{\pm} = |m_{\pm}| \exp(i\theta_{\pm})$. The first current in (C11) is CP even, while the latter is CP odd, and can be used to source baryogenesis. This latter term is there only when the source of CP violation, $\Delta\theta = \theta_+ - \theta_-$ does not vanish. The first term in the first equation is the (adiabatic) vacuum contribution (*i.e.* the leading classical term that would survive in the very thick wall limit).

Appendix D: Mode function normalization

In this appendix we shall show that the properly normalized mode functions that solve Eqs. (32), and whose indices are (33), are given by Eq. (34). Since a_{\pm}, b_{\pm}, c in Eq. (33) are non-integer, the two independent solutions for $\chi_{\pm h}$ are the usual ones, and they are of the form

$$\begin{aligned} u_{\pm h}^{(1)} &= u_{\pm h0}^{(1)} z^{\alpha} (1-z)^{\beta} \times {}_2F_1(a_{\pm}, b_{\pm}; c; z) \\ u_{\pm h}^{(2)} &= u_{\pm h0}^{(2)} z^{\alpha+1-c} (1-z)^{\beta} \times {}_2F_1(a_{\pm} + 1 - c, b_{\pm} + 1 - c; 2 - c; z) \\ &= u_{\pm h0}^{(2)} z^{\alpha+1-c} (1-z)^{\beta+c-a_{\pm}-b_{\pm}} \times {}_2F_1(1 - a_{\pm}, 1 - b_{\pm}; 2 - c; z), \end{aligned} \quad (\text{D1})$$

where $u_{\pm h0}^{(1,2)}$ are the normalisation z -independent constants (which we shall determine below) and ${}_2F_1(a, b; c; z)$ denotes the Gauss' hypergeometric function, whose series around $z = 0$ reads,

$${}_2F_1(a, b; c; z) = 1 + \frac{ab}{c}z + \frac{a(a+1)b(b+1)}{c(c+1)} \frac{z^2}{2!} + \dots + \frac{\Gamma(a+n)\Gamma(b+n)\Gamma(c)}{\Gamma(a)\Gamma(b)\Gamma(c+n)} \frac{z^n}{n!} + \dots$$

Notice that we have picked the sign of α and β in (30) such that the first (second) fundamental solution in Eqs. (D1) corresponds to the positive (negative) frequency wave at early times. Notice further that the solutions for $v_{\pm h}^{(1,2)} = u_{\pm h}^{(1,2)}$ are obtained simply by flipping the helicity h in $u_{\pm h}^{(1,2)}$. The latter form for of the two solutions (D1) is useful in that the prefactor is in the form $\alpha + 1 - c = -\alpha = \alpha^*$, $\beta + c - a_{\pm} - b_{\pm} = -\beta = \beta^*$. It then follows that, in the vicinity of $t \rightarrow -\infty$ ($z \rightarrow e^{2\gamma t}$), $u_{\pm h}^{(1)}$ and $u_{\pm h}^{(2)}$ reduce to the positive and negative frequency solutions, respectively,

$$u_{\pm h}^{(1)} \approx u_{\pm h0}^{(1)} e^{2\gamma\alpha t} = u_{\pm h0}^{(1)} e^{-i\omega_- t}, \quad u_{\pm h}^{(2)} \approx u_{\pm h0}^{(2)} e^{-2\gamma\alpha t} = u_{\pm h0}^{(2)} e^{i\omega_- t} \quad (t \rightarrow -\infty, z \rightarrow e^{2\gamma t}). \quad (\text{D2})$$

In analogy to what we did in Eq. (A9), here we shall take the positive frequency solution at $t \rightarrow -\infty$, *i.e.* $u_{\pm h} = u_{\pm h}^{(1)}$. Due to the fact that the vacua at $t \rightarrow -\infty$ and $t \rightarrow +\infty$ are not the same (they are related by a Bogoliubov transformation), the positive frequency solution becomes a mixture of positive and negative frequency solutions close to $t \rightarrow +\infty$, as can be implied from the following identity (see *e.g.* Eq. (9.131.1-2) of Ref. [63]),

$$\begin{aligned} {}_2F_1(a_{\pm}, b_{\pm}; c; z) &= \frac{\Gamma(c)\Gamma(c - a_{\pm} - b_{\pm})}{\Gamma(c - a_{\pm})\Gamma(c - b_{\pm})} \times {}_2F_1(a_{\pm}, b_{\pm}; a_{\pm} + b_{\pm} + 1 - c; 1 - z) \\ &+ \frac{\Gamma(c)\Gamma(a_{\pm} + b_{\pm} - c)}{\Gamma(a_{\pm})\Gamma(b_{\pm})} (1 - z)^{c - a_{\pm} - b_{\pm}} \times {}_2F_1(c - a_{\pm}, c - b_{\pm}; c + 1 - a_{\pm} - b_{\pm}; 1 - z). \end{aligned} \quad (\text{D3})$$

Indeed, we have,

$$\begin{aligned} u_{\pm h} \equiv u_{\pm h}^{(1)} &= u_{\pm h0} z^{\alpha} (1 - z)^{\beta} \times \frac{\Gamma(c)\Gamma(c - a_{\pm} - b_{\pm})}{\Gamma(c - a_{\pm})\Gamma(c - b_{\pm})} \times {}_2F_1(a_{\pm}, b_{\pm}; a_{\pm} + b_{\pm} + 1 - c; 1 - z) \\ &+ u_{\pm h0} \frac{\Gamma(c)\Gamma(a_{\pm} + b_{\pm} - c)}{\Gamma(a_{\pm})\Gamma(b_{\pm})} z^{\alpha} (1 - z)^{\beta+c-a_{\pm}-b_{\pm}} \times {}_2F_1(c - a_{\pm}, c - b_{\pm}; c + 1 - a_{\pm} - b_{\pm}; 1 - z), \end{aligned} \quad (\text{D4})$$

from which we infer that in the vicinity of $t \rightarrow \infty$ ($z \rightarrow 1 - e^{-2\gamma t}$),

$$u_{\pm h} \approx u_{\pm h0} \frac{\Gamma(c)\Gamma(c-a_{\pm}-b_{\pm})}{\Gamma(c-a_{\pm})\Gamma(c-b_{\pm})} e^{-i\omega_{\pm}t} + u_{\pm h0} \frac{\Gamma(c)\Gamma(a_{\pm}+b_{\pm}-c)}{\Gamma(a_{\pm})\Gamma(b_{\pm})} e^{i\omega_{\pm}t} \quad (t \rightarrow \infty, 1-z \rightarrow e^{-2\gamma t}), \quad (D5)$$

where we made use of $\tilde{c} \equiv a_{\pm} + b_{\pm} + 1 - c = 1 + 2\beta$, $\beta + c - a_{\pm} - b_{\pm} = \beta + 1 - \tilde{c} = -\beta$.

One can also construct late time positive and negative frequency solutions that solve the differential equation (32). Equation (D4) implies that, if (D1) are solutions, so must be both parts of Eq. (D4), such that the two linearly independent late time solutions are,

$$\begin{aligned} \tilde{u}_{\pm h}^{(1)} &= \tilde{u}_{\pm h0}^{(2)} z^{\alpha} (1-z)^{\beta+1-\tilde{c}} \times {}_2F_1(a_{\pm}+1-\tilde{c}, b_{\pm}+1-\tilde{c}; 2-\tilde{c}; 1-z) \\ &= \tilde{u}_{\pm h0}^{(2)} z^{\alpha+\tilde{c}-a_{\pm}-b_{\pm}} (1-z)^{\beta+1-\tilde{c}} \times {}_2F_1(1-a_{\pm}, 1-b_{\pm}; 2-\tilde{c}; 1-z) \\ \tilde{u}_{\pm h}^{(2)} &= \tilde{u}_{\pm h0}^{(1)} z^{\alpha} (1-z)^{\beta} \times {}_2F_1(a_{\pm}, b_{\pm}; \tilde{c}; 1-z) \quad (\tilde{c} = 1 + 2\beta), \end{aligned} \quad (D6)$$

where $\tilde{u}_{\pm h0}^{(1,2)}$ are normalisation constants. Now, because $\alpha + 1 - c = -\alpha = \alpha^*$ and $\beta + c - a_{\pm} - b_{\pm} = -\beta = \beta^*$, the asymptotic forms for the mode functions are,

$$\tilde{u}_{\pm h}^{(1)} \approx \tilde{u}_{\pm h0}^{(1)} e^{-i\omega_{\pm}t}, \quad \tilde{u}_{\pm h}^{(2)} \approx \tilde{u}_{\pm h0}^{(2)} e^{i\omega_{\pm}t} \quad (t \rightarrow \infty, 1-z \rightarrow e^{-2\gamma t}). \quad (D7)$$

One can check that Eqs. (D6) indeed solve Eq. (32), so they constitute legitimate linearly independent solutions for the mode functions. And moreover, each of the solutions (D6) can be written as a linear combination of the early time solutions (D1), as they should.

Next, we need to properly normalize our mode functions (D1) and (D6). Rather than performing a quantum mechanical normalization such as was used in [56], we shall use the field theoretic normalization (11–13), since it is more suitable for baryogenesis applications we have in mind. Since u_{+h} and u_{-h} are related by a first order differential equations (22), their normalisation constants are not independent. Let us begin by rewriting (22) as

$$\left[z(1-z) \frac{d}{dz} \pm i \frac{m_{1R} + m_{2R}(1-2z)}{2\gamma} \right] u_{\pm h} = i \frac{hk \pm im_I}{2\gamma} u_{\mp h}. \quad (D8)$$

By making use of the identities,

$$\alpha = \frac{c-1}{2}; \quad \beta = \frac{a_{\pm} + b_{\pm} - c}{2}; \quad \pm \frac{im_{2R}}{2\gamma} = \frac{1 + b_{\pm} - a_{\pm}}{4}; \quad \pm \frac{im_{1R}}{2\gamma} = \frac{(a_{\pm} + b_{\pm} - 1)(a_{\pm} + b_{\pm} + 1 - 2c)}{4(a_{\pm} - 1 - b_{\pm})}$$

we can recast Eq. (D8) as

$$\left[z(1-z) \frac{d}{dz} + \frac{b_{\pm}(a_{\pm} - c)}{a_{\pm} - 1 - b_{\pm}} - b_{\pm}z \right] u_{\pm h0} \times {}_2F_1(a_{\pm}, b_{\pm}; c; z) = i \frac{hk \pm im_I}{2\gamma} u_{\mp h0} \times {}_2F_1(a_{\pm} - 1, b_{\pm} + 1; c; z), \quad (D9)$$

where we used $a_{\mp} = b_{\pm} + 1$ and $b_{\mp} = a_{\pm} - 1$. In order to transform the parameters of the hypergeometric function on the left hand side such to correspond to those on the right hand side, let us first make use of the following two identities (see Eq. (9.137.6) and (9.137.17) in [63]),

$$\begin{aligned} \frac{d}{dz} ({}_2F_1(a, b; c; z)) &= \frac{ab}{c} \times {}_2F_1(a+1, b+1; c+1; z) \\ \frac{abz}{c} \times {}_2F_1(a+1, b+1; c+1; z) &= (c-1) \left[{}_2F_1(a, b; c-1; z) - {}_2F_1(a, b; c; z) \right], \end{aligned} \quad (D10)$$

upon which Eq. (D9) reduces to

$$\begin{aligned} \left[(1-z)(c-1) \times {}_2F_1(a_{\pm}, b_{\pm}; c-1; z) + \left(\frac{b_{\pm}(a_{\pm} - c)}{a_{\pm} - 1 - b_{\pm}} - c + 1 + (c-1-b_{\pm})z \right) \times {}_2F_1(a_{\pm}, b_{\pm}; c; z) \right] u_{\pm h0} \\ = i \frac{hk \pm im_I}{2\gamma} u_{\mp h0} \times {}_2F_1(a_{\pm} - 1, b_{\pm} + 1; c; z). \end{aligned} \quad (D11)$$

This can be further transformed by making use of (9.137.17) in [63],

$$(c-1) \times {}_2F_1(a, b; c-1; z) = b \times {}_2F_1(a, b+1; c; z) + (c-1-b) \times {}_2F_1(a, b; c; z) \quad (D12)$$

into

$$\left[(1-z)b_{\pm} \times {}_2F_1(a_{\pm}, b_{\pm}+1; c; z) + \frac{b_{\pm}(b_{\pm}+1-c)}{a_{\pm}-1-b_{\pm}} \times {}_2F_1(a_{\pm}, b_{\pm}; c; z) \right] u_{\pm h0} \quad (D13)$$

$$= i \frac{hk \pm im_I}{2\gamma} u_{\mp h0} \times {}_2F_1(a_{\pm}-1, b_{\pm}+1; c; z).$$

We need one more transformation [71],

$$(1-z)(a-b-1) \times {}_2F_1(a, b+1; c; z) = (a-c) \times {}_2F_1(a-1, b+1; c; z) + (c-1-b) \times {}_2F_1(a, b; c; z), \quad (D14)$$

with which one gets on both sides of equation (D13) a function with identical parameters, implying the following relation between the normalisation constants

$$\frac{u_{\pm h0}}{u_{\mp h0}} = i \frac{hk \pm im_I}{2\gamma} \times \frac{a_{\pm} - b_{\pm} - 1}{b_{\pm}(a_{\pm} - c)}. \quad (D15)$$

Several comments are now in order. This expression shows that CP violation is in the relative phase between u_{+h} and u_{-h} solutions,

$$e^{i\theta_{CP\pm}} = \frac{hk \pm im_I}{\sqrt{k^2 + m_I^2}}, \quad (D16)$$

which was to be expected, meaning that there is no trace of CP violation in the parameters a_{\pm} , b_{\pm} or c of the hypergeometric functions. Moreover,

$$\frac{k^2 + m_I^2}{4\gamma^2} = \frac{b_{\pm}(a_{\pm}-1)(a_{\pm}-c)(b_{\pm}+1-c)}{(a_{\pm}-b_{\pm}-1)^2},$$

such that the ratio (D15) can be expressed in terms of the phase θ_{CP} and the parameters a_{\pm} , b_{\pm} and c ,

$$\frac{u_{\pm h0}}{u_{\mp h0}} = \pm \frac{hk \pm im_I}{\sqrt{k^2 + m_I^2}} \times \frac{\sqrt{-b_{\pm}(a_{\pm}-c)(a_{\pm}-1)(b_{\pm}+1-c)}}{b_{\pm}(a_{\pm}-c)} = -\frac{hk \pm im_I}{\sqrt{k^2 + m_I^2}} \times \sqrt{\frac{\omega_{-} \pm (m_{1R} + m_{2R})}{\omega_{-} \mp (m_{1R} + m_{2R})}}, \quad (D17)$$

where we made use of $(a_{\pm} - b_{\pm} - 1)^2 = -[\pm i(a_{\pm} - b_{\pm} - 1)^2] = -4m_{2R}^2/\gamma^2$ and in the last step,

$$b_{\pm}(a_{\pm} - c) = \mp \frac{[\omega_{-} \mp (m_{1R} + m_{2R})]m_{2R}}{\gamma^2}, \quad (a_{\pm} - 1)(b_{\pm} + 1 - c) = \pm \frac{[\omega_{-} \pm (m_{1R} + m_{2R})]m_{2R}}{\gamma^2}.$$

Eq. (D17) nicely separates the relative CP-violating phase between positive and negative frequency modes and their amplitude ratio which is not CP-violating. From Eq. (D16) it also follows that $\theta_{CP} \equiv \theta_{CP+} = -\theta_{CP-}$, *i.e.* that $e^{i\theta_{CP+}} e^{i\theta_{CP-}} = 1$.

What remains to be done is to perform normalisation of the mode functions. Eqs. (A8) and (21) imply for the early time mode functions (D1),

$$|u_{+h}|^2 + |u_{-h}|^2 = 1 = |v_{+h}|^2 + |v_{-h}|^2, \quad (D18)$$

and analogously for the late time mode functions (D6),

$$|\tilde{u}_{+h}|^2 + |\tilde{u}_{-h}|^2 = 1 = |\tilde{v}_{+h}|^2 + |\tilde{v}_{-h}|^2. \quad (D19)$$

Making use of (D17), the first condition in (D18) can be written as,

$$|u_{+h0}|^2 \left[{}_2F_1(a_{+}, b_{+}; c; z) \times {}_2F_1(2-a_{+}, -b_{+}; 2-c; z) - \frac{b_{+}(a_{+}-c)}{(a_{+}-1)(b_{+}+1-c)} \times {}_2F_1(a_{-}, b_{-}; c; z) \times {}_2F_1(2-a_{-}, -b_{-}; 2-c; z) \right] = 1, \quad (D20)$$

where we made use of the fact that α and β are purely imaginary, and of $a_{\pm}^* = 2 - a_{\pm}$, $b_{\pm}^* = -b_{\pm}$, $c^* = 2 - c$ and $z^* = z$ is real (the proper sign in front of the second term is a minus). Next, it is convenient to replace a_- and b_- by a_+ and b_+ ($b_- = a_+ - 1$, $a_- = b_+ + 1$) in the second term. The above analysis (see Eqs. (D9–D15)) implies

$$\left[\frac{a-b-1}{b(a-c)} z(1-z) \frac{d}{dz} + \left(1 - \frac{a-b-1}{a-c} z \right) \right] {}_2F_1(a, b; c; z) = {}_2F_1(a-1, b+1; c; z)$$

and also $(a \rightarrow 1-b, b \rightarrow 1-a, c \rightarrow 2-c)$,

$$\left[\frac{a-b-1}{(1-a)(c-b-1)} z(1-z) \frac{d}{dz} + \left(1 - \frac{a-b-1}{c-b-1} z \right) \right] {}_2F_1(1-b, 1-a; 2-c; z) = {}_2F_1(2-a, -b; 2-c; z).$$

The latter relation can be used to replace the second hypergeometric function on the first line in (D20), while the former to replace the first hypergeometric function ${}_2F_1(a_-, b_-; c; z) = {}_2F_1(a_+ - 1, b_+ + 1; c; z)$ in the second line of (D20) to obtain,

$$\begin{aligned} 1 = & |u_{+h0}|^2 \left\{ {}_2F_1(a_+, b_+; c; z) \left[\frac{a_+ - b_+ - 1}{(1-a_+)(c-b_+-1)} z(1-z) \frac{d}{dz} + \left(1 - \frac{a_+ - b_+ - 1}{c-b_+-1} z \right) \right] {}_2F_1(1-b_+, 1-a_+; 2-c; z) \right. \\ & \left. - \frac{b_+(a_+-c)}{(a_+-1)(b_++1-c)} \left[\frac{a_+ - b_+ - 1}{b_+(a_+-c)} z(1-z) \frac{d}{dz} + \left(1 - \frac{a_+ - b_+ - 1}{a_+-c} z \right) \right] {}_2F_1(a_+, b_+; c; z) \times {}_2F_1(1-a_+, 1-b_+; 2-c; z) \right\}. \end{aligned} \quad (D21)$$

Next we can make use of the Wronskian for the hypergeometric functions,

$$W[{}_2F_1(a, b; c; z), z^{1-c}(1-z)^{c-a-b} {}_2F_1(1-a, 1-b; 2-c; z)] = (1-c)z^{-c}(1-z)^{c-a-b-1}, \quad (D22)$$

from which it follows that,

$$W[{}_2F_1(a, b; c; z), {}_2F_1(1-a, 1-b; 2-c; z)] + {}_2F_1(a, b; c; z) \left(\frac{1-c}{z} - \frac{c-b-a}{1-z} \right) {}_2F_1(1-a, 1-b; 2-c; z) = \frac{1-c}{z(1-z)}. \quad (D23)$$

When this is inserted into (D21) many terms cancel and one ends up with,

$$|u_{+h0}|^2 = \frac{(1-a_+)(c-b_+-1)}{(a_+-b_+-1)(1-c)} = \frac{\omega_- + (m_{1R} + m_{2R})}{2\omega_-}. \quad (D24)$$

To summarize, we have found that the normalized early time mode functions (D1) are (cf. Eq. (D17)),

$$\begin{aligned} u_{+h} &\equiv u_{+h}^{(1)} = \sqrt{\frac{\omega_- + (m_{1R} + m_{2R})}{2\omega_-}} \times z^\alpha (1-z)^\beta \times {}_2F_1(a_+, b_+; c; z) \\ u_{-h} &\equiv u_{-h}^{(1)} = -\frac{hk - im_I}{\sqrt{k^2 + m_I^2}} \times \sqrt{\frac{\omega_- - (m_{1R} + m_{2R})}{2\omega_-}} \times z^\alpha (1-z)^\beta \times {}_2F_1(a_-, b_-; c; z), \end{aligned} \quad (D25)$$

which are also given in Eqs. (34). An analogous procedure yields two other normalised mode functions given in Eqs. (35–37).

Appendix E: Connecting the kink wall to the thin wall case

Here we shall show that the early and late time solutions for the mode functions for a tanh wall profile are equivalent to those for the thin wall case in the limit $\gamma \rightarrow \infty$. Similarly, we shall demonstrate the agreement between the Bogoliubov coefficients α and β and the corresponding particle number.

The early time solutions for the tanh wall (34) reduce in the limit $\gamma \rightarrow \infty$ to

$$\begin{aligned} u_{+h} &\equiv u_{+h}^{(1)} \xrightarrow{\gamma \rightarrow \infty} \sqrt{\frac{\omega_- + m_{-R}}{2\omega_-}} \times e^{-i\omega_- t} \\ u_{-h} &\equiv u_{-h}^{(1)} \xrightarrow{\gamma \rightarrow \infty} -\frac{hk - im_I}{\sqrt{k^2 + m_I^2}} \times \sqrt{\frac{\omega_- - m_{-R}}{2\omega_-}} \times e^{-i\omega_- t}, \end{aligned} \quad (E1)$$

where $m_{-R} = m_{1R} + m_{2R}$ and $m_- = m_{-R} + im_{1I}$ is the mass for $t < 0$. The same result can be obtained by solving Eqs. (22) for constant mass $m_R = m_{-R}$ and choosing the positive frequency solution at early time, $u_{\pm h} = u_{\pm h0}e^{-i\omega_-t}$. After normalisation according to $|u_{+h}|^2 + |u_{-h}|^2 = 1$ the result (E1) is found. If we solve similarly Eqs. (22) for the negative frequency solution at early time, $v_{\pm h} = v_{\pm h0}e^{i\omega_-t}$, we find that

$$\begin{aligned} v_{+h} &\equiv u_{+(-h)}^{(2)} \xrightarrow{\gamma \rightarrow \infty} \sqrt{\frac{\omega_- - m_{-R}}{2\omega_-}} \times e^{i\omega_-t} \\ v_{-h} &\equiv u_{-(-h)}^{(2)} \xrightarrow{\gamma \rightarrow \infty} -\frac{hk + im_I}{\sqrt{k^2 + m_I^2}} \times \sqrt{\frac{\omega_- + m_{-R}}{2\omega_-}} \times e^{i\omega_-t}. \end{aligned} \quad (E2)$$

In order to compare to the thin wall solutions at early time Eqs. (A9) we should rotate back to the L_h, R_h basis from the $u_{\pm h}$ basis. By making use of (21) and the solutions (E1–E2) we compute

$$\begin{aligned} L_h^- &= \frac{\omega_- - hk + m_-}{\sqrt{4\omega_-(\omega_- + m_{-R})}} e^{-i\omega_-t}, & R_h^- &= \frac{\omega_- + hk + m_-^*}{\sqrt{4\omega_-(\omega_- + m_{-R})}} e^{-i\omega_-t} \\ \bar{L}_h^- &= \frac{\omega_- - hk - m_-}{\sqrt{4\omega_-(\omega_- - m_{-R})}} e^{i\omega_-t}, & \bar{R}_h^- &= \frac{\omega_- + hk - m_-^*}{\sqrt{4\omega_-(\omega_- - m_{-R})}} e^{i\omega_-t}. \end{aligned} \quad (E3)$$

At first sight these solutions do not seem to be consistent with Eqs. (A9). However, they can be rewritten as

$$\begin{aligned} L_h^- &= \sqrt{\frac{\omega_- - hk}{2\omega_-}} e^{i\theta_L} e^{-i\omega_-t}, & R_h^- &= \sqrt{\frac{\omega_- + hk}{2\omega_-}} e^{i\theta_R} e^{-i\omega_-t} \\ \bar{L}_h^- &= -\sqrt{\frac{\omega_- - hk}{2\omega_-}} e^{i\theta_{\bar{L}}} e^{i\omega_-t}, & \bar{R}_h^- &= \sqrt{\frac{\omega_- + hk}{2\omega_-}} e^{i\theta_{\bar{R}}} e^{i\omega_-t}, \end{aligned} \quad (E4)$$

where the (real) phases are given by

$$\begin{aligned} \theta_L &= \arctan\left(\frac{m_I}{\omega_- - hk + m_{-R}}\right), & \theta_R &= \arctan\left(\frac{-m_I}{\omega_- + hk + m_{-R}}\right) \\ \theta_{\bar{L}} &= \arctan\left(\frac{-m_I}{\omega_- - hk - m_{-R}}\right), & \theta_{\bar{R}} &= \arctan\left(\frac{m_I}{\omega_- + hk - m_{-R}}\right). \end{aligned} \quad (E5)$$

Thus the early time mode functions L_h are R_h in the thin wall limit (E3) only differ from those computed directly for the thin wall (B3) by a common phase factor. A further global $U(1)$ rotation of the L_h, R_h spinor χ_h by $e^{-i\theta_L}$, and of the \bar{L}_h, \bar{R}_h spinor ν_h by $e^{i(\pi - \theta_L)}$, reduces the solutions (E4) to those in Eq. (A9). Here we used that

$$e^{i(\theta_R - \theta_L)} = \frac{m_-^*}{|m_-|} = e^{i(\bar{\theta}_R - \bar{\theta}_L)}, \quad (E6)$$

which follows from the identity $\arctan(x) - \arctan(y) = \arctan((x - y)/(1 + xy))$.

Next step is to check the late time solutions. Since the general late time solution for the mode functions is a linear combination of the fundamental late time solutions $\tilde{u}_{\pm h}^{(1)}$ and $\tilde{u}_{\pm h}^{(2)}$ given in Eqs. (36–37), we should consider both in the thin wall limit $\gamma \rightarrow \infty$. Eq. (38) now becomes

$$\begin{aligned} \tilde{u}_{+h} &= \alpha_{+h} \tilde{u}_{+h}^{(1)} + \beta_{+h} \tilde{u}_{+h}^{(2)} \\ &\xrightarrow{\gamma \rightarrow \infty} \alpha_{+h} \sqrt{\frac{\omega_+ + m_{+R}}{2\omega_+}} e^{-i\omega_+t} + \beta_{+h} \sqrt{\frac{\omega_+ - m_{+R}}{2\omega_+}} e^{i\omega_+t} \\ \tilde{u}_{-h} &= \alpha_{-h} \tilde{u}_{-h}^{(1)} + \beta_{-h} \tilde{u}_{-h}^{(2)} \\ &\xrightarrow{\gamma \rightarrow \infty} -\alpha_{-h} \frac{hk - im_I}{\sqrt{k^2 + m_I^2}} \sqrt{\frac{\omega_+ - m_{+R}}{2\omega_+}} e^{-i\omega_+t} + \beta_{-h} \frac{hk - im_I}{\sqrt{k^2 + m_I^2}} \sqrt{\frac{\omega_+ + m_{+R}}{2\omega_+}} e^{i\omega_+t}. \end{aligned} \quad (E7)$$

The thin wall limit for the Bogoliubov coefficients (41) is (see also (44)):

$$\begin{aligned} \alpha_{\pm h} &= \sqrt{\frac{\omega_+[\omega_- \pm (m_{1R} + m_{2R})]}{\omega_-[\omega_+ \pm (m_{1R} - m_{2R})]}} \frac{\omega_- + \omega_+ \mp 2m_{2R}}{2\omega_+} \\ \beta_{\pm h} &= \pm \sqrt{\frac{\omega_+[\omega_- \pm (m_{1R} + m_{2R})]}{\omega_-[\omega_+ \mp (m_{1R} - m_{2R})]}} \frac{\omega_+ - \omega_- \pm 2m_{2R}}{2\omega_+}. \end{aligned} \quad (E8)$$

Thus the coefficients are real and they can be shown to satisfy (42). The late time solutions for L_h and R_h can be derived via Eq. (21) from the solutions (E7),

$$\begin{aligned} L_h^+ &= \alpha_{+h} \frac{\omega_+ - hk + m_+}{\sqrt{4\omega_+(\omega_+ + m_{+R})}} e^{-i\omega_+ t} + \beta_{+h} \frac{\omega_+ + hk - m_+}{\sqrt{4\omega_+(\omega_+ - m_{+R})}} e^{i\omega_+ t} \\ R_h^+ &= \alpha_{+h} \frac{\omega_+ + hk + m_+^*}{\sqrt{4\omega_+(\omega_+ + m_{+R})}} e^{-i\omega_+ t} + \beta_{+h} \frac{\omega_+ - hk - m_+^*}{\sqrt{4\omega_+(\omega_+ - m_{+R})}} e^{i\omega_+ t}. \end{aligned} \quad (\text{E9})$$

As for the solutions for $t < 0$, we also write the late time solutions in a form more similar to (B4). This gives

$$\begin{aligned} L_h^+ &= \alpha_{+h} \sqrt{\frac{\omega_+ - hk}{2\omega_+}} e^{i\theta_L^{(1)}} e^{-i\omega_+ t} + \beta_{+h} \sqrt{\frac{\omega_+ - hk}{2\omega_+}} e^{i\theta_L^{(2)}} e^{i\omega_+ t} \\ R_h^+ &= \alpha_{+h} \sqrt{\frac{\omega_+ + hk}{2\omega_+}} e^{i\theta_R^{(1)}} e^{-i\omega_+ t} + \beta_{+h} \sqrt{\frac{\omega_+ + hk}{2\omega_+}} e^{i\theta_R^{(2)}} e^{i\omega_+ t}. \end{aligned} \quad (\text{E10})$$

The corresponding phase factors are

$$\begin{aligned} \theta_L^{(1)} &= \arctan\left(\frac{m_I}{\omega_+ - hk + m_{+R}}\right), & \theta_R^{(1)} &= \arctan\left(\frac{-m_I}{\omega_+ + hk + m_{+R}}\right) \\ \theta_L^{(2)} &= \arctan\left(\frac{-m_I}{\omega_+ + hk - m_{+R}}\right), & \theta_R^{(2)} &= \arctan\left(\frac{m_I}{\omega_+ - hk - m_{+R}}\right). \end{aligned} \quad (\text{E11})$$

We have seen that the early time solutions for L_h, R_h in the thin wall limit, Eqs. (E4), differ from those computed directly for the thin wall (A9) by a global phase factor. This factor could be removed by rotating the particle spinor by a factor of $e^{-i\theta_L}$. Since the general late time solution matches the early time one, this means that also the late time solution should be rotated by the same factor. The resulting phase factor for the α_{+h} and β_{+h} solutions should match the phase factor present in the solutions (B4). Indeed we can show that

$$\begin{aligned} \theta_L^{(1)} - \theta_L &= \text{Arg}[\alpha_h^+] \\ \theta_R^{(1)} - \theta_L &= \text{Arg}[\alpha_h^+] + \arctan\left(\frac{-m_I}{m_{+R}}\right) \\ \theta_L^{(2)} - \theta_L &= \text{Arg}[\beta_h^+] \\ \theta_R^{(2)} - \theta_L &= \text{Arg}[\beta_h^+] + \arctan\left(\frac{-m_I}{m_{+R}}\right), \end{aligned} \quad (\text{E12})$$

where the α_h^+ and β_h^+ on the righthand side are the ones in Eq. (B6). The conclusion we therefore make is the following: although the Bogoliubov coefficients computed by taking the thin wall limit of the kink wall solutions (E8) appear different from those directly computed for the thin wall (B6), they in fact only differ by a global phase factor, which does not affect the particle number. In the thin wall limit computations, the Bogoliubov coefficients (E8) are real, but the early and late time mode functions carry a global phase factor, see Eqs. (E5) and (E11). In the direct thin wall computations, the (coefficients of) the mode functions do not carry the global phase factor, see (B3) and (B4), but the global phase is present in the Bogoliubov coefficients (B6), which are hence complex. In any case, global rotations of the (anti)particle spinors are always allowed, and such rotations simply move the phase factor back and forth between Bogoliubov coefficients and mode functions, leading to physically equivalent solutions.

Appendix F: Deriving the kinetic and constraint equations in gradient approximation

In this section we derive the kinetic and constraint equations for the densities g_{ah} . Our starting point is Eq. (73) with the *Ansatz* (51). After inserting $\gamma^0\gamma^0 = 1$ in front of $iS^{+-}(k; x)$ in Eq. (73), we get,

$$\begin{aligned} \left\{ (I \otimes I) k^0 - \rho^3 \otimes (\vec{k} \cdot \vec{\sigma}) + \frac{i}{2} (I \otimes I) \partial_t - m_R(t) (\rho^1 \otimes I) \exp\left(-\frac{i}{2} \overleftarrow{\partial}_t \overrightarrow{\partial}_{k_0}\right) - m_I(t) (\rho^2 \otimes I) \exp\left(-\frac{i}{2} \overleftarrow{\partial}_t \overrightarrow{\partial}_{k_0}\right) \right\} \\ \times (\rho^a g_{ah}(\vec{k}; x)) \otimes \frac{1}{4} (1 + h\hat{k} \cdot \vec{\sigma}) = 0, \end{aligned} \quad (\text{F1})$$

where we made use of the Bloch representation of the Clifford algebra, in which

$$\gamma^0 \rightarrow \rho^1 \otimes I; \quad \gamma^i \rightarrow \rho^2 \otimes \sigma^i; \quad \gamma^5 \rightarrow -\rho^3 \otimes I; \quad \hat{H} = \hat{k} \cdot \gamma^0 \vec{\gamma} \gamma^5 \rightarrow \hat{k} \cdot I \otimes \vec{\sigma}. \quad (\text{F2})$$

Now, upon multiplying from the left by

$$\{I, h\gamma^i \gamma^5, -\imath h\gamma^i, -\gamma^5\} \rightarrow \{I \otimes I, \rho^1 \otimes h\sigma^i, \rho^2 \otimes h\sigma^i, \rho^3 \otimes I\},$$

and taking a trace, we get the following four equations,

$$k_0 g_{0h} - h k g_{3h} + \frac{\imath}{2} \partial_t g_{0h} - m_R(t) \exp\left(-\frac{\imath}{2} \overleftarrow{\partial}_t \overrightarrow{\partial}_{k_0}\right) g_{1h} - m_I(t) \exp\left(-\frac{\imath}{2} \overleftarrow{\partial}_t \overrightarrow{\partial}_{k_0}\right) g_{2h} = 0 \quad (\text{F3})$$

$$k_0 g_{1h} + \imath h k g_{2h} + \frac{\imath}{2} \partial_t g_{1h} - m_R(t) \exp\left(-\frac{\imath}{2} \overleftarrow{\partial}_t \overrightarrow{\partial}_{k_0}\right) g_{0h} - \imath m_I(t) \exp\left(-\frac{\imath}{2} \overleftarrow{\partial}_t \overrightarrow{\partial}_{k_0}\right) g_{3h} = 0 \quad (\text{F4})$$

$$k_0 g_{2h} - \imath h k g_{1h} + \frac{\imath}{2} \partial_t g_{2h} + \imath m_R(t) \exp\left(-\frac{\imath}{2} \overleftarrow{\partial}_t \overrightarrow{\partial}_{k_0}\right) g_{3h} - m_I(t) \exp\left(-\frac{\imath}{2} \overleftarrow{\partial}_t \overrightarrow{\partial}_{k_0}\right) g_{0h} = 0 \quad (\text{F5})$$

$$k_0 g_{3h} - h k g_{0h} + \frac{\imath}{2} \partial_t g_{3h} - \imath m_R(t) \exp\left(-\frac{\imath}{2} \overleftarrow{\partial}_t \overrightarrow{\partial}_{k_0}\right) g_{2h} + \imath m_I(t) \exp\left(-\frac{\imath}{2} \overleftarrow{\partial}_t \overrightarrow{\partial}_{k_0}\right) g_{1h} = 0. \quad (\text{F6})$$

Now, hermiticity of $\imath \gamma^0 S^{+-}$ implies reality of the component functions g_{ah} , such that the real and imaginary parts of Eqs. (F3–F6) must be separately satisfied. The real parts yield constraint equations (CEs),

$$k_0 g_{0h} - h k g_{3h} - m_R(t) \cos\left(\frac{1}{2} \overleftarrow{\partial}_t \overrightarrow{\partial}_{k_0}\right) g_{1h} - m_I(t) \cos\left(\frac{1}{2} \overleftarrow{\partial}_t \overrightarrow{\partial}_{k_0}\right) g_{2h} = 0 \quad (\text{F7})$$

$$k_0 g_{1h} - m_R(t) \cos\left(\frac{1}{2} \overleftarrow{\partial}_t \overrightarrow{\partial}_{k_0}\right) g_{0h} - m_I(t) \sin\left(\frac{1}{2} \overleftarrow{\partial}_t \overrightarrow{\partial}_{k_0}\right) g_{3h} = 0 \quad (\text{F8})$$

$$k_0 g_{2h} + m_R(t) \sin\left(\frac{1}{2} \overleftarrow{\partial}_t \overrightarrow{\partial}_{k_0}\right) g_{3h} - m_I(t) \cos\left(\frac{1}{2} \overleftarrow{\partial}_t \overrightarrow{\partial}_{k_0}\right) g_{0h} = 0 \quad (\text{F9})$$

$$k_0 g_{3h} - h k g_{0h} - m_R(t) \sin\left(\frac{1}{2} \overleftarrow{\partial}_t \overrightarrow{\partial}_{k_0}\right) g_{2h} + m_I(t) \sin\left(\frac{1}{2} \overleftarrow{\partial}_t \overrightarrow{\partial}_{k_0}\right) g_{1h} = 0, \quad (\text{F10})$$

while the imaginary parts yield the following kinetic equations (KEs),

$$\partial_t g_{0h} + 2m_R(t) \sin\left(\frac{1}{2} \overleftarrow{\partial}_t \overrightarrow{\partial}_{k_0}\right) g_{1h} + 2m_I(t) \sin\left(\frac{1}{2} \overleftarrow{\partial}_t \overrightarrow{\partial}_{k_0}\right) g_{2h} = 0 \quad (\text{F11})$$

$$\partial_t g_{1h} + 2h k g_{2h} + 2m_R(t) \sin\left(\frac{1}{2} \overleftarrow{\partial}_t \overrightarrow{\partial}_{k_0}\right) g_{0h} - 2m_I(t) \cos\left(\frac{1}{2} \overleftarrow{\partial}_t \overrightarrow{\partial}_{k_0}\right) g_{3h} = 0 \quad (\text{F12})$$

$$\partial_t g_{2h} - 2h k g_{1h} + 2m_R(t) \cos\left(\frac{1}{2} \overleftarrow{\partial}_t \overrightarrow{\partial}_{k_0}\right) g_{3h} + 2m_I(t) \sin\left(\frac{1}{2} \overleftarrow{\partial}_t \overrightarrow{\partial}_{k_0}\right) g_{0h} = 0 \quad (\text{F13})$$

$$\partial_t g_{3h} - 2m_R(t) \cos\left(\frac{1}{2} \overleftarrow{\partial}_t \overrightarrow{\partial}_{k_0}\right) g_{2h} + 2m_I(t) \cos\left(\frac{1}{2} \overleftarrow{\partial}_t \overrightarrow{\partial}_{k_0}\right) g_{1h} = 0. \quad (\text{F14})$$

Due to the nonlocal nature of the derivative operators, these equations are hard to solve, and hence not very useful. However, when truncated at a finite number of derivatives ∂_t , they reduce to a set of relatively simple equations. This derivative truncation, which is a generalization of the quantum mechanical WKB expansion, holds when formally

$$\hbar \|\partial_t\| \ll |k_0|, \quad (\text{F15})$$

where we reinserted \hbar to make it explicit that this derivative expansion is in fact an expansion in powers of \hbar . Note that no matter how large the norm $\|\partial_t\|$, there always will be modes that satisfy the criterion (F15). Conversely, no matter how slow the changes in time are, there always will be modes that break (F15). In some sense, the criterion (F15) divides a theory into two parts: the semiclassical part where (F15) holds and the quantum part, where (F15) is broken. Of course, a full quantum mechanical kink wall treatment is required for those modes that break condition (F15), while a semiclassical treatment should suffice when (F15) is satisfied. When modes are massive on both sides of the wall, then the theory has a gap of $2\min[|m(t)|]$, and – at least on-shell – $|k_0| \geq \min[|m(t)|]$.⁶

⁶ When interactions (loops) are included, due to quantum effects the mass gap can decrease, or even completely disappear, so one should be careful when making statements concerning applicability of the gradient approximation, even in the case when the tree level mass is present on both sides of the ‘wall’. For example, in the case of the electroweak phase transition, it is typically the case that the tree level mass, and hence the gap, is zero on the symmetric side of the bubble wall.

While the classical kinetic theory is obtained by keeping the CEs up to 0th order in derivatives and kinetic equations to first order in derivatives, in order to get semiclassical equations which contain information on CP violation require to maintain first order derivatives in the CEs and second order derivatives in the KEs. Let us now consider the constraint equations (F7–F10). We have

$$g_{1h} = \frac{m_R(t)}{k_0} \cos\left(\frac{1}{2} \overleftarrow{\partial}_t \overrightarrow{\partial}_{k_0}\right) g_{0h} + \frac{m_I(t)}{k_0} \sin\left(\frac{1}{2} \overleftarrow{\partial}_t \overrightarrow{\partial}_{k_0}\right) g_{3h} \quad (\text{F16})$$

$$g_{2h} = -\frac{m_R(t)}{k_0} \sin\left(\frac{1}{2} \overleftarrow{\partial}_t \overrightarrow{\partial}_{k_0}\right) g_{3h} + \frac{m_I(t)}{k_0} \cos\left(\frac{1}{2} \overleftarrow{\partial}_t \overrightarrow{\partial}_{k_0}\right) g_{0h}. \quad (\text{F17})$$

Upon inserting these into Eqs. (F7) and (F10), and truncating to first order in derivatives, we get

$$\frac{k_0^2 - m_R^2 - m_I^2}{k_0} g_{0h} - \left[hk + \frac{m_R \partial_t m_I - m_I \partial_t m_R}{2k_0} \partial_{k_0} \right] g_{3h} = 0 \quad (\text{F18})$$

$$k_0 g_{3h} - \left[hk - \frac{m_R \partial_t m_I - m_I \partial_t m_R}{2} \partial_{k_0} \frac{1}{k_0} \right] g_{0h} = 0. \quad (\text{F19})$$

These two equations can be easily decoupled, such that (again to first order in gradients) we have

$$\left(k_0^2 - |m|^2 - k^2 \right) g_{0h} = 0 \quad (\text{F20})$$

$$\left(k_0^2 - |m|^2 - k^2 - hk \frac{|m|^2 \dot{\theta}}{k_0^2 - |m|^2} \right) g_{3h} = 0, \quad (\text{F21})$$

where we used a shorthand notation,

$$|m|^2 = m_R^2 + m_I^2; \quad m_R = |m| \cos(\theta); \quad m_I = |m| \sin(\theta); \quad |m|^2 \dot{\theta} = m_R \partial_t m_I - m_I \partial_t m_R.$$

Eqs. (F20) and (F21) are presented in the main text, see (74) and (75). Next we consider the kinetic equations to second order in gradients. First we treat the kinetic equations for g_{0h} and g_{3h} , in order to describe CP violation in the axial vector current. So, we begin by inserting Eqs. (F16–F17) into Eqs. (F11) and (F14), and we get

$$\partial_t g_{0h} + \frac{\partial_t |m|^2}{2} \partial_{k_0} \frac{g_{0h}}{k_0} = 0 \quad (\text{F22})$$

$$\partial_t g_{3h} + \frac{\partial_t |m|^2}{2k_0} \partial_{k_0} g_{3h} - \frac{\partial_t (|m|^2 \partial_t \theta)}{4} \left(\partial_{k_0}^2 - \frac{1}{k_0} \partial_{k_0}^2 k_0 \right) \frac{g_{0h}}{k_0} = 0, \quad (\text{F23})$$

where we made use of

$$m_R \partial_t m_R + m_I \partial_t m_I = \frac{1}{2} \partial_t |m|^2; \quad m_R \partial_t^2 m_I - m_I \partial_t^2 m_R = \partial_t (|m|^2 \partial_t \theta). \quad (\text{F24})$$

Now, upon making use of $g_{0h} = (hk_0/k)g_{3h}$ plus higher orders (*cf.* Eq. (F18)) and pulling k_0 to the left of the derivatives, Eq. (F23) simplifies to,

$$\partial_t g_{3h} + \frac{\partial_t |m|^2}{2k_0} \partial_{k_0} g_{3h} + h \frac{\partial_t (|m|^2 \partial_t \theta)}{2k_0} \partial_{k_0} g_{3h} = 0. \quad (\text{F25})$$

These are presented in the main text in (78) and (79).

Additionally, we can solve the constraint and kinetic equations for g_{1h} and g_{2h} . In a similar procedure as before, we first take the CEs (F7) and (F10), and combine them to find

$$\begin{aligned} 0 &= (k_0^2 - k^2) g_{0h} - k_0 m_R \cos\left(\frac{1}{2} \overleftarrow{\partial}_t \overrightarrow{\partial}_{k_0}\right) g_{1h} + h k m_I \sin\left(\frac{1}{2} \overleftarrow{\partial}_t \overrightarrow{\partial}_{k_0}\right) g_{1h} - k_0 m_I \cos\left(\frac{1}{2} \overleftarrow{\partial}_t \overrightarrow{\partial}_{k_0}\right) g_{2h} - h k m_R \sin\left(\frac{1}{2} \overleftarrow{\partial}_t \overrightarrow{\partial}_{k_0}\right) g_{2h} \\ 0 &= (k_0^2 - k^2) g_{3h} + k_0 m_I \sin\left(\frac{1}{2} \overleftarrow{\partial}_t \overrightarrow{\partial}_{k_0}\right) g_{1h} - h k m_R \cos\left(\frac{1}{2} \overleftarrow{\partial}_t \overrightarrow{\partial}_{k_0}\right) g_{1h} - k_0 m_R \sin\left(\frac{1}{2} \overleftarrow{\partial}_t \overrightarrow{\partial}_{k_0}\right) g_{2h} - h k m_I \cos\left(\frac{1}{2} \overleftarrow{\partial}_t \overrightarrow{\partial}_{k_0}\right) g_{2h}. \end{aligned} \quad (\text{F26})$$

Now, by making use of these equations we can eliminate g_{0h} and g_{3h} from the remaining constraint equations (F8) and (F9). After an expansion up to second order in derivatives ∂_{k_0} we find,

$$\begin{aligned} & \frac{k_0^2 - k^2 - m_R^2}{k_0^2 - k^2} k_0 g_{1h} + hk \left[\frac{m_R \dot{m}_I}{2} \frac{1}{k_0^2 - k^2} \partial_{k_0} - \frac{m_R \dot{m}_I}{2} \partial_{k_0} \frac{1}{k_0^2 - k^2} \right] g_{1h} \\ & + \left[\frac{\ddot{m}_R m_R}{8} \partial_{k_0}^2 \frac{k_0}{k_0^2 - k^2} + \frac{\ddot{m}_R m_R}{8} \frac{k_0}{k_0^2 - k^2} \partial_{k_0}^2 + \frac{1}{4} \dot{m}_I^2 \partial_{k_0} \frac{k_0}{k_0^2 - k^2} \partial_{k_0} \right] g_{1h} \\ & - \frac{m_I m_R}{k_0^2 - k^2} k_0 g_{2h} + hk \left[-\frac{m_R \dot{m}_I}{2} \frac{1}{k_0^2 - k^2} \partial_{k_0} - \frac{m_I \dot{m}_I}{2} \partial_{k_0} \frac{1}{k_0^2 - k^2} \right] g_{2h} \\ & + \left[\frac{\ddot{m}_R m_I}{8} \partial_{k_0}^2 \frac{k_0}{k_0^2 - k^2} + \frac{\ddot{m}_R m_I}{8} \frac{k_0}{k_0^2 - k^2} \partial_{k_0}^2 - \frac{1}{4} \dot{m}_I \dot{m}_R \partial_{k_0} \frac{k_0}{k_0^2 - k^2} \partial_{k_0} \right] g_{2h} = 0 \end{aligned} \quad (\text{F27})$$

$$\begin{aligned} & \frac{k_0^2 - k^2 - m_I^2}{k_0^2 - k^2} k_0 g_{2h} + hk \left[-\frac{m_I \dot{m}_R}{2} \frac{1}{k_0^2 - k^2} \partial_{k_0} + \frac{m_I \dot{m}_R}{2} \partial_{k_0} \frac{1}{k_0^2 - k^2} \right] g_{2h} \\ & + \left[\frac{\ddot{m}_I m_I}{8} \partial_{k_0}^2 \frac{k_0}{k_0^2 - k^2} + \frac{\ddot{m}_I m_I}{8} \frac{k_0}{k_0^2 - k^2} \partial_{k_0}^2 + \frac{1}{4} \dot{m}_R^2 \partial_{k_0} \frac{k_0}{k_0^2 - k^2} \partial_{k_0} \right] g_{2h} \\ & - \frac{m_I m_R}{k_0^2 - k^2} k_0 g_{1h} + hk \left[\frac{m_I \dot{m}_I}{2} \frac{1}{k_0^2 - k^2} \partial_{k_0} + \frac{m_R \dot{m}_R}{2} \partial_{k_0} \frac{1}{k_0^2 - k^2} \right] g_{1h} \\ & + \left[\frac{\ddot{m}_I m_R}{8} \partial_{k_0}^2 \frac{k_0}{k_0^2 - k^2} + \frac{\ddot{m}_I m_R}{8} \frac{k_0}{k_0^2 - k^2} \partial_{k_0}^2 - \frac{1}{4} \dot{m}_I \dot{m}_R \partial_{k_0} \frac{k_0}{k_0^2 - k^2} \partial_{k_0} \right] g_{1h} = 0. \end{aligned} \quad (\text{F28})$$

As is mentioned above it is only necessary to solve the constraint equations to first order in gradients in order to describe CP violation. The reason for expanding to second order will become clear once we discuss the kinetic equations. For now we take the constraint equations (F27)–(F28) only to first order in gradients and proceed with a description of the decoupling procedure.

After multiplying Eq. (F27) with $k_0^2 - k^2 - m_I^2$ and adding $m_I m_R$ times (F28), the zeroth order contribution in g_{2h} drops out. Thus, this gives the zeroth order shell for g_{1h} , which follows from

$$\frac{k_0}{k_0^2 - k^2} [(k_0^2 - k^2 - m_R^2)(k_0^2 - k^2 - m_I^2) - m_I^2 m_R^2] g_{1h} = k_0(k_0^2 - k^2 - |m|^2) g_{1h}.$$

Similarly, we can find the zeroth order shell for g_{2h} . Although the constraint equations are now decoupled at zeroth order, both g_{1h} and g_{2h} still contribute at first order. However, at this point we may use the zeroth order relation between g_{2h} and g_{1h} . From Eqs. (F27) and (F28) it can be seen that $g_{2h} = [m_I m_R / (k_0^2 - k^2 - m_I^2)] g_{1h}$ and $g_{1h} = [m_I m_R / (k_0^2 - k^2 - m_R^2)] g_{2h}$, respectively. Inserting the first in the constraint equation for g_{1h} , and the latter in the constraint equation for g_{2h} (both decoupled at zeroth order), one obtains

$$\left(k_0^2 - k^2 - |m|^2 + hk \frac{\dot{m}_I}{m_R} \right) g_{1h} = 0 \quad (\text{F29})$$

$$\left(k_0^2 - k^2 - |m|^2 - hk \frac{\dot{m}_R}{m_I} \right) g_{2h} = 0. \quad (\text{F30})$$

Note that the first order derivatives ∂_{k_0} have been canceled. The solutions for g_{1h} and g_{2h} are

$$g_{1h} = \tilde{g}_{1h} 2\pi\delta \left(k_0^2 - k^2 - |m|^2 + hk \frac{\dot{m}_I}{m_R} \right) \quad (\text{F31})$$

$$g_{2h} = \tilde{g}_{2h} 2\pi\delta \left(k_0^2 - k^2 - |m|^2 - hk \frac{\dot{m}_R}{m_I} \right). \quad (\text{F32})$$

Thus, like the axial density g_{3h} , also g_{1h} and g_{2h} live on shifted energy shells

$$\omega_{1h} = \omega_0 - hk \frac{\dot{m}_I}{2\omega_0 m_R}, \quad \omega_{2h} = \omega_0 + hk \frac{\dot{m}_R}{2\omega_0 m_I}, \quad (\text{F33})$$

where ω_0 is presented in (77). Note that the CP-odd part can be shown more explicitly by writing

$$\omega_{1h} = \omega_0 - hk \frac{\dot{\theta}}{2\omega_0} - hk \tan \theta \frac{|\dot{m}|}{2\omega_0 |m|}, \quad \omega_{2h} = \omega_0 + hk \frac{\dot{\theta}}{2\omega_0} - hk \cot \theta \frac{|\dot{m}|}{2\omega_0 |m|}.$$

CP violation is present due to the changing phase of the mass.

We continue with the kinetic equations (F12) and (F13). Also here we eliminate g_{0h} and g_{3h} in favor of g_{1h} and g_{2h} and we expand to second order in gradients. The result is

$$\begin{aligned} & \partial_t g_{1h} - 2hk \frac{m_I m_R}{k_0^2 - k^2} g_{1h} + \left[m_I \dot{m}_I \frac{k_0}{k_0^2 - k^2} \partial_{k_0} + m_R \dot{m}_R \partial_{k_0} \frac{k_0}{k_0^2 - k^2} \right] g_{1h} \\ & + 2hk \left[\frac{\ddot{m}_R m_I}{8} \partial_{k_0}^2 \frac{1}{k_0^2 - k^2} + \frac{\ddot{m}_R m_I}{8} \frac{1}{k_0^2 - k^2} \partial_{k_0}^2 - \frac{\dot{m}_R \dot{m}_I}{4} \partial_{k_0} \frac{1}{k_0^2 - k^2} \partial_{k_0} \right] g_{1h} \\ & + 2hk \frac{k_0^2 - k^2 - m_I^2}{k_0^2 - k^2} g_{2h} + \left[-m_I \dot{m}_R \frac{k_0}{k_0^2 - k^2} \partial_{k_0} + m_I \dot{m}_R \partial_{k_0} \frac{k_0}{k_0^2 - k^2} \right] g_{2h} \\ & + 2hk \left[\frac{\ddot{m}_I m_I}{8} \partial_{k_0}^2 \frac{1}{k_0^2 - k^2} + \frac{\ddot{m}_I m_I}{8} \frac{1}{k_0^2 - k^2} \partial_{k_0}^2 + \frac{1}{4} \dot{m}_R \dot{m}_I \partial_{k_0} \frac{k_0}{k_0^2 - k^2} \partial_{k_0} \right] g_{2h} = 0 \end{aligned} \quad (\text{F34})$$

$$\begin{aligned} & \partial_t g_{2h} + 2hk \frac{m_I m_R}{k_0^2 - k^2} g_{2h} + \left[m_R \dot{m}_R \frac{k_0}{k_0^2 - k^2} \partial_{k_0} + m_I \dot{m}_I \partial_{k_0} \frac{k_0}{k_0^2 - k^2} \right] g_{2h} \\ & - 2hk \left[\frac{\ddot{m}_R m_I}{8} \partial_{k_0}^2 \frac{1}{k_0^2 - k^2} + \frac{\ddot{m}_I m_R}{8} \frac{1}{k_0^2 - k^2} \partial_{k_0}^2 - \frac{\dot{m}_I \dot{m}_R}{4} \partial_{k_0} \frac{1}{k_0^2 - k^2} \partial_{k_0} \right] g_{2h} \\ & - 2hk \frac{k_0^2 - k^2 - m_R^2}{k_0^2 - k^2} g_{1h} + \left[-m_R \dot{m}_I \frac{k_0}{k_0^2 - k^2} \partial_{k_0} + m_R \dot{m}_I \partial_{k_0} \frac{k_0}{k_0^2 - k^2} \right] g_{1h} \\ & - 2hk \left[\frac{\ddot{m}_R m_R}{8} \partial_{k_0}^2 \frac{1}{k_0^2 - k^2} + \frac{\ddot{m}_R m_R}{8} \frac{1}{k_0^2 - k^2} \partial_{k_0}^2 + \frac{1}{4} \dot{m}_I \dot{m}_I \partial_{k_0} \frac{k_0}{k_0^2 - k^2} \partial_{k_0} \right] g_{1h} = 0. \end{aligned} \quad (\text{F35})$$

At this point we can use the constraint equations (F27)–(F28) to replace some of the zeroth order terms in Eqs. (F34)–(F35) by terms of higher order in derivatives. The remaining terms in the equations above are the zeroth order terms $\partial_t g_{1h}$ and $\partial_t g_{2h}$ plus a mix of first and second order terms in g_{1h} and g_{2h} . In the same fashion as was done for the constraint equations, we can eliminate the *first* order terms for g_{2h} from the kinetic equation for g_{1h} by inserting the *first* order solutions for g_{2h} from Eq. (F28) (vice versa for the kinetic equation for g_{2h}). Then we eliminate the remaining *second* order terms for g_{2h} by using the *zeroth* order terms for g_{2h} from Eq. (F28) (similarly for the second kinetic equation). In the resulting kinetic equations for g_{1h} and g_{2h} all double derivatives $\partial_{k_0}^2$ have dropped out. The result is

$$\partial_t g_{1h} + \frac{\partial_t |m|^2}{2k_0} \partial_{k_0} g_{1h} + \left[-\frac{m_R \dot{m}_R}{k_0^2 - k^2 - m_I^2} + \frac{hk m_R \ddot{m}_I}{(k_0^2 - k^2 - m_I^2)^2} \right] g_{1h} - \frac{hk m_R^2 \partial_t (\dot{m}_I / m_R)}{2k_0 (k_0^2 - k^2 - m_I^2)} \partial_{k_0} g_{1h} = 0 \quad (\text{F36})$$

$$\partial_t g_{2h} + \frac{\partial_t |m|^2}{2k_0} \partial_{k_0} g_{2h} + \left[-\frac{m_I \dot{m}_I}{k_0^2 - k^2 - m_R^2} - \frac{hk m_I \ddot{m}_R}{(k_0^2 - k^2 - m_R^2)^2} \right] g_{2h} + \frac{hk m_I^2 \partial_t (\dot{m}_R / m_I)}{2k_0 (k_0^2 - k^2 - m_R^2)} \partial_{k_0} g_{2h} = 0. \quad (\text{F37})$$

The kinetic equations for g_{1h} and g_{2h} can be integrated over k_0 to obtain kinetic equations for the phase space densities f_{1h} and f_{2h} . By making use of the solutions (F32) one obtains

$$\partial_t \ln(f_{1h}) = \partial_t \ln \left(\frac{m_R}{\omega_{1h}} \right) \quad (\text{F38})$$

$$\partial_t \ln(f_{2h}) = \partial_t \ln \left(\frac{m_I}{\omega_{1h}} \right). \quad (\text{F39})$$

These equations are easily solved with initial conditions (67), and the solutions are

$$f_{1h}(t) = -\frac{m_R(t)}{\omega_{1h}(t)} (1 - 2\bar{n}_{th}) \quad (\text{F40})$$

$$f_{2h}(t) = -\frac{m_I}{\omega_{2h}(t)} (1 - 2\bar{n}_{th}). \quad (\text{F41})$$

Thus, we have found the phase space densities f_{1h} and f_{2h} in the gradient approximation, including CP violating effects. It can be shown that f_{1h} and f_{2h} from Eqs. (F40)–(F41), together with the solution for f_{3h} (85) and $f_{0h} = 1$, satisfy the kinetic equations (53) to the given order in gradient approximation.

As a final note we mention that the authors of Refs. [64–70] have developed a formalism that takes account

of the existence of an additional shell at $k_0 = 0$, which is permitted by the constraint equations. For this shell the constraint equations can be solved up to zeroth order in the gradient expansion, and its solutions carry information on quantum coherence. Note that the $k_0 = 0$ shell seems to be outside the validity of the gradient approximation (F15). However, a more general condition for the gradient expansion is $\hbar \|\partial_t \partial_{k_0}\| \ll 1$, for which the $k_0 = 0$ shell can be incorporated. It is interesting that collective phenomena in the plasma can generate a feature that resembles the $k_0 = 0$ shell (see figures 13 and 14 in Ref. [72]). However there are also differences; in the weakly coupled regime one sees a double peak structure centered around $k_0 = 0$, which as coupling increases merge into one broad shell centered around $k_0 = 0$. This feature is probably not related to the quantum coherent shell at $k_0 = 0$ since it is not generated by quantum coherence, but instead by collective plasma phenomena.

-
- [1] D. E. Morrissey and M. J. Ramsey-Musolf, “Electroweak baryogenesis,” *New J. Phys.* **14** (2012) 125003 [arXiv:1206.2942 [hep-ph]].
 - [2] K. Kajantie, M. Laine, K. Rummukainen and M. E. Shaposhnikov, “A Nonperturbative analysis of the finite T phase transition in $SU(2) \times U(1)$ electroweak theory,” *Nucl. Phys. B* **493** (1997) 413 [hep-lat/9612006].
 - [3] K. Rummukainen, M. Tsybin, K. Kajantie, M. Laine and M. E. Shaposhnikov, “The Universality class of the electroweak theory,” *Nucl. Phys. B* **532** (1998) 283 [hep-lat/9805013].
 - [4] F. Csikor, Z. Fodor and J. Heitger, “Endpoint of the hot electroweak phase transition,” *Phys. Rev. Lett.* **82** (1999) 21 [hep-ph/9809291].
 - [5] M. Carena, G. Nardini, M. Quiros and C. E. M. Wagner, “The Baryogenesis Window in the MSSM,” *Nucl. Phys. B* **812** (2009) 243 [arXiv:0809.3760 [hep-ph]].
 - [6] M. Pospelov and A. Ritz, “Electric dipole moments as probes of new physics,” *Annals Phys.* **318** (2005) 119 [arXiv:hep-ph/0504231].
 - [7] M. Carena, G. Nardini, M. Quiros and C. E. M. Wagner, “MSSM Electroweak Baryogenesis and LHC Data,” arXiv:1207.6330 [hep-ph].
 - [8] K. Blum and Y. Nir, “Beyond MSSM Baryogenesis,” *Phys. Rev. D* **78** (2008) 035005 [arXiv:0805.0097 [hep-ph]].
 - [9] T. Konstandin, T. Prokopec, M. G. Schmidt and M. Seco, “MSSM electroweak baryogenesis and flavor mixing in transport equations,” *Nucl. Phys. B* **738** (2006) 1 [hep-ph/0505103].
 - [10] V. Cirigliano, Y. Li, S. Profumo and M. J. Ramsey-Musolf, “MSSM Baryogenesis and Electric Dipole Moments: An Update on the Phenomenology,” *JHEP* **1001** (2010) 002 [arXiv:0910.4589 [hep-ph]].
 - [11] J. M. Cline, M. Joyce and K. Kainulainen, “Supersymmetric electroweak baryogenesis,” *JHEP* **0007** (2000) 018 [arXiv:hep-ph/0006119]. J. M. Cline, M. Joyce and K. Kainulainen, “Supersymmetric electroweak baryogenesis. (Erratum),” arXiv:hep-ph/0110031.
 - [12] P. Huet and A. E. Nelson, “Electroweak baryogenesis in supersymmetric models,” *Phys. Rev. D* **53** (1996) 4578 [hep-ph/9506477].
 - [13] J. Kozaczuk, S. Profumo, M. J. Ramsey-Musolf and C. L. Wainwright, “Supersymmetric Electroweak Baryogenesis Via Resonant Sfermion Sources,” *Phys. Rev. D* **86** (2012) 096001 [arXiv:1206.4100 [hep-ph]].
 - [14] V. Cirigliano, C. Lee and S. Tulin, “Resonant Flavor Oscillations in Electroweak Baryogenesis,” *Phys. Rev. D* **84** (2011) 056006 [arXiv:1106.0747 [hep-ph]].
 - [15] T. Konstandin, T. Prokopec and M. G. Schmidt, “Kinetic description of fermion flavor mixing and CP-violating sources for baryogenesis,” *Nucl. Phys. B* **716** (2005) 373 [hep-ph/0410135].
 - [16] S. J. Huber and M. G. Schmidt, “Electroweak baryogenesis: Concrete in a SUSY model with a gauge singlet,” *Nucl. Phys. B* **606** (2001) 183 [hep-ph/0003122].
 - [17] J. Kang, P. Langacker, T. -j. Li and T. Liu, “Electroweak baryogenesis in a supersymmetric $U(1)$ -prime model,” *Phys. Rev. Lett.* **94** (2005) 061801 [hep-ph/0402086].
 - [18] M. Carena, N. R. Shah and C. E. M. Wagner, “Light Dark Matter and the Electroweak Phase Transition in the NMSSM,” *Phys. Rev. D* **85** (2012) 036003 [arXiv:1110.4378 [hep-ph]].
 - [19] T. Konstandin and S. J. Huber, “Numerical approach to multi dimensional phase transitions,” *JCAP* **0606** (2006) 021 [hep-ph/0603081].
 - [20] S. J. Huber and M. G. Schmidt, “SUSY variants of the electroweak phase transition,” *Eur. Phys. J. C* **10** (1999) 473 [hep-ph/9809506].
 - [21] J. M. Cline and K. Kainulainen, “Electroweak baryogenesis and dark matter from a singlet Higgs,” arXiv:1210.4196 [hep-ph].
 - [22] S. J. Huber, T. Konstandin, T. Prokopec and M. G. Schmidt, “Baryogenesis in the MSSM, nMSSM and NMSSM,” *Nucl. Phys. A* **785** (2007) 206 [hep-ph/0608017].
 - [23] S. J. Huber, T. Konstandin, T. Prokopec and M. G. Schmidt, “Electroweak Phase Transition and Baryogenesis in the nMSSM,” *Nucl. Phys. B* **757** (2006) 172 [hep-ph/0606298].
 - [24] C. Balazs, M. S. Carena, A. Freitas and C. E. M. Wagner, “Phenomenology of the nMSSM from colliders to cosmology,” *JHEP* **0706** (2007) 066 [arXiv:0705.0431 [hep-ph]].
 - [25] A. Menon, D. E. Morrissey and C. E. M. Wagner, “Electroweak baryogenesis and dark matter in the nMSSM,” *Phys. Rev. D* **70** (2004) 035005 [arXiv:hep-ph/0404184].

- [26] J. M. Cline, K. Kainulainen and M. Trott, “Electroweak Baryogenesis in Two Higgs Doublet Models and B meson anomalies,” *JHEP* **1111** (2011) 089 [arXiv:1107.3559 [hep-ph]].
- [27] L. Fromme, S. J. Huber and M. Seniuch, “Baryogenesis in the two-Higgs doublet model,” *JHEP* **0611** (2006) 038 [hep-ph/0605242].
- [28] J. R. Espinosa, B. Gripaio, T. Konstandin and F. Riva, “Electroweak Baryogenesis in Non-minimal Composite Higgs Models,” *JCAP* **1201** (2012) 012 [arXiv:1110.2876 [hep-ph]].
- [29] T. Konstandin and G. Servant, “Natural Cold Baryogenesis from Strongly Interacting Electroweak Symmetry Breaking,” *JCAP* **1107** (2011) 024 [arXiv:1104.4793 [hep-ph]].
- [30] J. M. Cline, M. Jarvinen and F. Sannino, “The Electroweak Phase Transition in Nearly Conformal Technicolor,” *Phys. Rev. D* **78** (2008) 075027 [arXiv:0808.1512 [hep-ph]].
- [31] A. Tranberg and B. Wu, “Cold Electroweak Baryogenesis in the Two Higgs-Doublet Model,” *JHEP* **1207** (2012) 087 [arXiv:1203.5012 [hep-ph]].
- [32] A. Tranberg and B. Wu, “On using Cold Baryogenesis to constrain the Two-Higgs Doublet Model,” arXiv:1210.1779 [hep-ph].
- [33] A. Tranberg, A. Hernandez, T. Konstandin and M. G. Schmidt, “Cold electroweak baryogenesis with Standard Model CP violation,” *Phys. Lett. B* **690** (2010) 207 [arXiv:0909.4199 [hep-ph]].
- [34] N. S. Manton, “Topology in the Weinberg-Salam Theory,” *Phys. Rev. D* **28** (1983) 2019.
- [35] F. R. Klinkhamer and N. S. Manton, “A Saddle Point Solution in the Weinberg-Salam Theory,” *Phys. Rev. D* **30** (1984) 2212.
- [36] T. Prokopec, M. G. Schmidt and S. Weinstock, “Transport equations for chiral fermions to order \hbar and electroweak baryogenesis. Part I,” *Annals Phys.* **314** (2004) 208 [hep-ph/0312110].
- [37] T. Prokopec, M. G. Schmidt and S. Weinstock, “Transport equations for chiral fermions to order \hbar and electroweak baryogenesis. Part II,” *Annals Phys.* **314** (2004) 267 [hep-ph/0406140].
- [38] A. G. Cohen, D. B. Kaplan and A. E. Nelson, “Baryogenesis at the weak phase transition,” *Nucl. Phys. B* **349** (1991) 727.
- [39] M. Joyce, T. Prokopec and N. Turok, “Efficient electroweak baryogenesis from lepton transport,” *Phys. Lett. B* **338** (1994) 269 [hep-ph/9401352].
- [40] M. Joyce, T. Prokopec and N. Turok, “Nonlocal electroweak baryogenesis. Part 1: Thin wall regime,” *Phys. Rev. D* **53** (1996) 2930 [hep-ph/9410281].
- [41] M. Joyce, T. Prokopec and N. Turok, “Electroweak baryogenesis from a classical force,” *Phys. Rev. Lett.* **75** (1995) 1695 [Erratum-ibid. **75** (1995) 3375] [arXiv:hep-ph/9408339].
- [42] M. Joyce, T. Prokopec and N. Turok, “Nonlocal electroweak baryogenesis. Part 2: The Classical regime,” *Phys. Rev. D* **53** (1996) 2958 [hep-ph/9410282].
- [43] M. Joyce, K. Kainulainen and T. Prokopec, “The Semiclassical propagator in field theory,” *Phys. Lett. B* **468** (1999) 128 [hep-ph/9906411].
- [44] G. R. Farrar and M. E. Shaposhnikov, “Baryon asymmetry of the universe in the standard electroweak theory,” *Phys. Rev. D* **50** (1994) 774 [hep-ph/9305275].
- [45] M. B. Gavela, M. Lozano, J. Orloff and O. Pene, “Standard model CP violation and baryon asymmetry. Part 1: Zero temperature,” *Nucl. Phys. B* **430** (1994) 345 [hep-ph/9406288].
- [46] M. B. Gavela, P. Hernandez, J. Orloff, O. Pene and C. Quimbay, “Standard model CP violation and baryon asymmetry. Part 2: Finite temperature,” *Nucl. Phys. B* **430** (1994) 382 [hep-ph/9406289].
- [47] P. Huet and E. Sather, “Electroweak baryogenesis and standard model CP violation,” *Phys. Rev. D* **51** (1995) 379 [hep-ph/9404302].
- [48] K. Kainulainen, T. Prokopec, M. G. Schmidt and S. Weinstock, “First principle derivation of semiclassical force for electroweak baryogenesis,” *JHEP* **0106** (2001) 031 [hep-ph/0105295].
- [49] K. Kainulainen, T. Prokopec, M. G. Schmidt and S. Weinstock, “Semiclassical force for electroweak baryogenesis: Three-dimensional derivation,” *Phys. Rev. D* **66** (2002) 043502 [hep-ph/0202177].
- [50] A. Riotto, *Nucl. Phys. B* **518** (1998) 339 [hep-ph/9712221].
- [51] M. S. Carena, M. Quiros, A. Riotto, I. Vilja and C. E. M. Wagner, “Electroweak baryogenesis and low-energy supersymmetry,” *Nucl. Phys. B* **503** (1997) 387 [hep-ph/9702409].
- [52] M. S. Carena, J. M. Moreno, M. Quiros, M. Seco and C. E. M. Wagner, “Supersymmetric CP violating currents and electroweak baryogenesis,” *Nucl. Phys. B* **599** (2001) 158 [hep-ph/0011055].
- [53] V. Cirigliano, C. Lee, M. J. Ramsey-Musolf and S. Tulin, “Flavored Quantum Boltzmann Equations,” *Phys. Rev. D* **81** (2010) 103503 [arXiv:0912.3523 [hep-ph]].
- [54] G. D. Moore and T. Prokopec, “Bubble wall velocity in a first order electroweak phase transition,” *Phys. Rev. Lett.* **75** (1995) 777 [hep-ph/9503296].
- [55] G. D. Moore and T. Prokopec, “How fast can the wall move? A Study of the electroweak phase transition dynamics,” *Phys. Rev. D* **52** (1995) 7182 [hep-ph/9506475].
- [56] A. Ayala, J. Jalilian-Marian, L. D. McLerran and A. P. Vischer, “Scattering in the presence of electroweak phase transition bubble walls,” *Phys. Rev. D* **49** (1994) 5559 [hep-ph/9311296].
- [57] K. Funakubo, A. Kakuto, S. Otsuki, K. Takenaga and F. Toyoda, “Fermion scattering off a CP violating electroweak bubble wall. 2,” hep-ph/9407207.
- [58] B. Garbrecht and T. Prokopec, “Fermion mass generation in de Sitter space,” *Phys. Rev. D* **73** (2006) 064036 [gr-qc/0602011].
- [59] B. Garbrecht, T. Prokopec, M. G. Schmidt, “Particle number in kinetic theory,” *Eur. Phys. J. C* **38** (2004) 135-143.

- [hep-th/0211219].
- [60] B. Garbrecht, T. Prokopec and M. G. Schmidt, “Coherent baryogenesis,” *Phys. Rev. Lett.* **92** (2004) 061303 [hep-ph/0304088].
 - [61] B. Garbrecht, T. Prokopec and M. G. Schmidt, “SO(10)-GUT coherent baryogenesis,” *Nucl. Phys. B* **736** (2006) 133 [hep-ph/0509190].
 - [62] T. Prokopec, M. G. Schmidt and J. Weenink, “The Gaussian entropy of fermionic systems,” *Annals Phys.* **327** (2012) 3138 [arXiv:1204.4124 [hep-th]].
 - [63] Gradshteyn and Ryzhik, “Table of Integrals, Series, and Products” Alan Jeffrey and Daniel Zwillinger (eds.) Seventh edition (Feb 2007), ISBN number: 0-12-373637-4.
 - [64] C. Fidler, M. Herranen, K. Kainulainen and P. M. Rahkila, “Flavoured quantum Boltzmann equations from cQPA,” *JHEP* **1202** (2012) 065 [arXiv:1108.2309 [hep-ph]].
 - [65] M. Herranen, K. Kainulainen and P. M. Rahkila, “Flavour-coherent propagators and Feynman rules: Covariant cQPA formulation,” *JHEP* **1202** (2012) 080 [arXiv:1108.2371 [hep-ph]].
 - [66] M. Herranen, K. Kainulainen and P. M. Rahkila, “Coherent quantum Boltzmann equations from cQPA,” *JHEP* **1012** (2010) 072 [arXiv:1006.1929 [hep-ph]].
 - [67] M. Herranen, K. Kainulainen and P. M. Rahkila, “Coherent quasiparticle approximation (cQPA) and nonlocal coherence,” *J. Phys. Conf. Ser.* **220** (2010) 012007 [arXiv:0912.2490 [hep-ph]].
 - [68] M. Herranen, K. Kainulainen and P. M. Rahkila, “Kinetic transport theory with quantum coherence,” *Nucl. Phys. A* **820** (2009) 203C [arXiv:0811.0936 [hep-ph]].
 - [69] M. Herranen, K. Kainulainen and P. M. Rahkila, “Quantum kinetic theory for fermions in temporally varying backgrounds,” *JHEP* **0809** (2008) 032 [arXiv:0807.1435 [hep-ph]].
 - [70] M. Herranen, K. Kainulainen and P. M. Rahkila, “Towards a kinetic theory for fermions with quantum coherence,” *Nucl. Phys. B* **810** (2009) 389 [arXiv:0807.1415 [hep-ph]].
 - [71] The Wolfram Functions Site, <http://functions.wolfram.com/>.
 - [72] J. F. Koksma, T. Prokopec and M. G. Schmidt, “Decoherence in an Interacting Quantum Field Theory: Thermal Case,” *Phys. Rev. D* **83**, 085011 (2011) [arXiv:1102.4713 [hep-th]].